Universiteit Utrecht

Opleiding Natuur- en Sterrenkunde

Charging dynamics of a supercapacitor: a multiple-stack model studied by Poisson-Nernst-Planck equations and equivalent RC circuits.

Bachelor Thesis

Mikel Unibaso Berrueta

Supervisors:

Prof. Dr. René Van Roij
Institute for Theoretical Physics

Dr. Cheng Lian
Institute for Theoretical Physics

June 12, 2020

Abstract

In the last few years supercapacitors, high performance electricity storage systems, have attracted the attention of researchers due to the fundamental interest and wide range of applications. Carbon-based electrodes provide a larger capacitance thanks to their large surface area which has already been widely studied for the case of a single-plate capacitor. Hence, we have developed a new model trying to mimic the behaviour of a supercapacitor by a multiple-stack electrode-electrolyte system. We first analyse it solving Poisson-Nernst-Planck equations and by an equivalent equilibrium circuit model, with a sudden switching-on of the potential. Then, we go a step further in the circuit model to give solution for any time-dependent potential, though just a triangular periodic one is chosen to be studied within the thesis. Finally, we also make some simulations varying the geometry of the model.

Contents

1 Introduction **1**
1.1 Motivation 1
1.2 Previous Work 2

2 Theoretical Background **3**
2.1 Electric Double Layer (EDL) 3
2.2 Electrostatics in liquids 3
2.3 Transport phenomena 5
2.4 Poisson-Nernst-Planck equation 6
2.5 Multiple stack model 6

3 Single-plate capacitor **7**
3.1 Step function potential 7
3.1.1 Analytical Solutions 7
3.1.2 Circuit modelling 10
3.2 Time dependent potential 12

4 General Electrode-Electrolyte System. **15**
4.1 First approach to matrix notation by example case n=2 15
4.1.1 Step function potential 15
4.1.2 Time-dependent potential 19
4.2 General case 21
4.2.1 Analytical solutions using step- potential 21
4.2.2 Circuit modelling for the step potential 24
4.2.3 Circuit modelling for the time-dependent potential 27

5 Conclusions and discussion. **33**
5.1 Outlook 34

6 Acknowledgment **35**

A Appendix **I**
A.1 Solution to PNP equation for the single-plate capacitor I
A.2 Solution to differential equation IV
A.3 Integrating final solution V
A.4 General solutions to the step-function potential V
A.5 Solutions to time-dependent potential VII

1 Introduction

1.1 Motivation

In the 1950s, the company General Electric started analysing porous carbon electrodes in order to design capacitors with a huge effective surface area [1]. As is widely known from basic electrostatics, the energy E stored in a capacitor of capacitance C equals,

$$E = \frac{1}{2} C \psi^2, \tag{1}$$

where ψ refers to the applied voltage. For a parallel plate capacitor, the capacitance has the form

$$C = \frac{\epsilon A}{d}, \tag{2}$$

with ϵ the dielectric constant of the region in between, A the area of the plates, and d their separation distance. Thus, collected energy in such capacitor for a given potential increases linearly with the area,

$$E = \frac{\epsilon}{2d} A \psi^2. \tag{3}$$

Not long later, in 1957 H.Becker developed a "Low voltage electrolytic capacitor with porous carbon electrodes" and he wrote about it: "*It is not known exactly what takes place when the devices are used as energy storing devices, but tests have demonstrated that when used as a low voltage electrolytic capacitor, it exhibits an extremely high capacitance*"[2]. Structure that we will later discuss, double layer mechanism, was still unknown.

In 1999, Brian Evans Conway coined the term *supercapacitor* in order to refer to the system which was enable to store electrical charge due to previously mentioned double-layer and as result of reactions with pseudocapacitance charge transfer of ions between electrode and electrolyte. Our interest in studying such system comes from the fact that it is an energy harvesting method currently very demanded due to its applicability and increasingly being used for transport applications where rapid charging and discharging are required [3].

The relation among the porous structures and the charging dynamics of supercapacitors is poorly understood. Transmission line models ([4],[5],[6]) are capable to fit experimental data. Nonetheless, parameters therein do not have a direct interpretation in terms of microscopic properties of supercapacitors. Besides, at the moment molecular dynamics simulation ([7],[8],[9]), lattice Boltzmann simulations [10], and classical dynamic density functional theory [11] can give some insight about the charging mechanisms of a single or a few nanopores or a nanoscale anode-cathode model. However, predicted relaxation time scales are orders of magnitude smaller than experimentally measured [12]. Recently a new model to mimic the behaviour of carbon porous electrode has been developed by our research group, Soft Condensed Matter, from Utrecht University [13]. It mainly consist of many parallel planar electrodes in which ions of an electrolyte form electric double layers, topic that will be largely discusses below. Hence, our aim in this thesis is to study the charging dynamics of a

supercapacitor solving the proposed Poisson-Nernst-Planck equations that describe the ion dynamics and comparing it to the proposed equivalent equilibrium circuit model.

1.2 Previous Work

"*If I have seen further it is by standing on the shoulders of Giants.*" Isaac Newton 1675.

As any structure, knowledge is built up by adding pieces to an already existing base. Hence, any good work must rely on previous ones with the aim of keeping constructing under safe foundations. Therefore, before starting with the technical part of the thesis we would like to shortly comment which references have been crucial in order to carry out this research project.

To begin with I had to start diving into the topic by reading [14] which provided me a clear insight of the topic I was about to dive into. Thus, this is the main source from where we have extracted the needed information in order to develop a proper theoretical background, detailed in section 2.

Regarding to section 3, we have to cite these two works [13] and [15]. Both have been incredibly useful in order to set a consistent base from which first reproduce some calculations. On the one hand, the analytical solutions of the PNP equations were derived by following [15], however we managed to use our own development based on techniques from [16] and since we consider they might not be easy to follow for a Bachelor student, all the procedure done to solve them is fully detailed in Appendix A.1. On the other hand, information about RC equivalent circuit model has been extracted from [13] where the case of the sudden potential was studied.

Later on, we went ahead with some new ideas and questions that I, along with my both supervisors have come up with. One of them was the introduction of the so called cyclic voltammetry within our system the after reading [17].

2 Theoretical Background

In this section some useful theoretical analysis is presented as an introduction for the tools we shall use when dealing with the real physical system since we consider it is rather useful to built up a pre-knowledge on the topic.

2.1 Electric Double Layer (EDL)

To start with, the reader should have a qualitative idea about one of the most important features of the system, the formation of Electric Double Layer. This phenomenon occurs when a planar charged stack is placed in a electrolyte. Now you might wonder what an electrolyte is. Basically it is a substance that produces an electrically conducting solution when dissolved in a polar solvent, such as water. Regarding to electrolyte properties, it is known that some salts tend to dissociate spontaneously in liquids such us water, creating ions. By Thermodynamics we know spontaneous processes occur at constant T if the Helmholtz free energy is reduced. Due to the relation, $F = U - TS$, we actually know how electrostatics and entropy are involved in such processes. Basically, energy has to be done again their natural Coulomb interaction, so U must increase. Thus, dissociation should happen just if S increases as well. Created ions leave the surface (*counterions*) while the opposite charged ones stay bounded (*coions*). Due to the Second Law of Thermodynamics (i.e., for entropic reasons) they will have a tendency to distribute in the whole space as homogeneously as possible. Hence, the equilibrium between both opposing effects lead to the so called *electric double layer*. The typical distance between the EDL and the planar surface is called Debye length, commonly defined as follows:

$$\kappa^{-1} = \sqrt{\frac{\epsilon k_B T}{8\pi e^2 \rho_b}}. \tag{4}$$

with e being the standard notation for the charge of the electron, ρ_b the bulk density, k_B the Boltzmann constant and T the temperature of the system. This expression will be derived in the next section.

2.2 Electrostatics in liquids

We start our discussion of the charging dynamics of the supercapacitor by analysing the EDLs through the classical and perhaps the most simple example of the single charged wall in contact with electrolyte.
The starting point, it's of course, one of the fundamental laws in electrostatics, the so called Poisson equation,

$$\nabla^2 \psi(\mathbf{r}) = -\frac{4\pi}{\epsilon} Q(\mathbf{r}), \tag{5}$$

that relates the local charge density within the electrolyte, $Q(\mathbf{r})$, to the electric potential $\psi(\boldsymbol{r})$. Besides, it can actually be rewritten as $Q(z) = e(\rho_+(z) - \rho_-(z))$, with $\rho_\pm$ density of $\pm$ ions, due to the fact that our analysis is within a planar geometry in a x-y plane for

$z > 0$. In order to simplify, $\phi(z) = \frac{e\psi(z)}{k_B T}$ will be conveniently taken as dimensionless "effective potential" for the following derivations. Therefore Eq.(5) equation becomes

$$\partial_z^2 \phi(z) = -\frac{4\pi e^2}{\epsilon k_B T}(\rho_+(z) - \rho_-(z)). \tag{6}$$

Under equilibrium assumption we make an ansatz (which can be derived by the density functional theory as well) by approximating ionic densities by the so called Boltzmann distribution,

$$\rho_\pm(z) = \rho_b \exp(\mp\phi(z)). \tag{7}$$

By introducing the Boltzmann distribution to the Poisson equation, i.e., to Eq.(6), we get

$$\partial_z^2 \phi(z) = \kappa^2 \sinh \phi(z), \tag{8}$$

where κ^{-1}, is the so called Debye length previously given in Eq.(4). When dealing with second order differential equation two boundary conditions are required which are chosen to be the following

$$\begin{cases} \lim_{z\to\infty} \phi(z) = 0, \\ \phi(0^+) = -4\pi\lambda_B\sigma. \end{cases} \tag{9}$$

we conveniently introduce the so called Bjerrun length $\lambda_B = \frac{e^2}{\epsilon k_B T}$, which is property of the solvent and it is defined as the distance in which Coulomb interaction between two dissolved unit charges e equals $k_B T$.
The first condition comes from the fact that potential has to be finite at infinity and second due to the fact that we apply global charge neutrality so the total ionic charge must be opposite to the total charge on the surface, i.e,

$$\sigma = -\int_0^\infty Q(z)dz = \frac{4\pi e}{\epsilon}\phi'(z)\Big|_0^\infty = -\frac{4\pi e}{\epsilon}\phi'(0^+). \tag{10}$$

Thus, analytical solution to Eq.(8) along with the BC's from Eq.(9) is known as Gouy-Chapman solution (GCs)

$$\phi(z) = 2\ln\left[\frac{1+\gamma\exp(-\kappa z)}{1-\gamma\exp(-\kappa z)}\right]. \tag{11}$$

where $\gamma = \sqrt{(\frac{\kappa}{2\pi\lambda_B\sigma})^2 + 1} - \frac{\kappa}{2\pi\lambda_B\sigma}$, so that ionic densities:

$$\rho_\pm(z) = \rho_b\left[\frac{1\mp\gamma\exp(-\kappa z)}{1\pm\gamma\exp(-\kappa z)}\right]^2. \tag{12}$$

This analytic solution is interesting because should represent the limit for $z \to \infty$ of the time-dependent system results,i.e., when the distance between parallel plates within the capacitor goes to infinity.
For a fixed surface potential, $\phi(z = 0) = \phi_0$ at the electrode, γ takes the following form:

$$\gamma = \frac{e^{\frac{\phi_0}{2}} - 1}{e^{\frac{\phi_0}{2}} + 1},$$

then, the potential and profile densities are plotted for different values of ϕ_0:

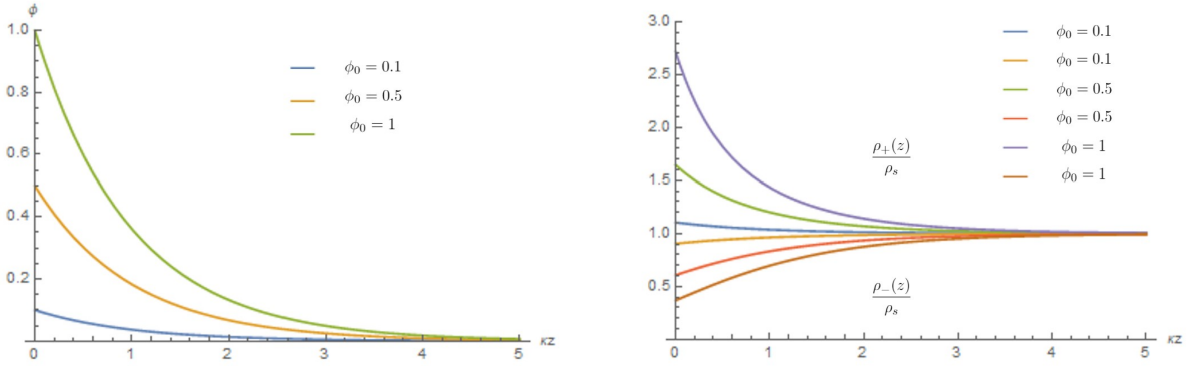

(a) (b)

Figure 1: Profiles of the dimensionless potential $\phi(z)$ (a) and ionic concentrations $\frac{\rho_\pm(z)}{\rho_s}$ (b) as a function of the dimensionless distance, κz, for a planar electrode with different values of ϕ_0.

Of course it is important to note that GCs does not describe the whole picture, there are cases in which ions are absorbed by the wall in which this solution is not valid anymore, however, under the assumptions we are interested in, it does work.

2.3 Transport phenomena

We consider an electrolyte flowing along charged surfaces and then notice that fluid can not only be driven by a pressure gradient but also by an electric field created due to a voltage difference, a phenomenon known as electro-osmosis (motion of liquid induced by an applied potential across a porous material, significant when in small channels). As a general remark, let us assume our system has i species of z_i valency, with ϵ dielectric constant η viscosity, T temperature and it is in contact with electrodes. We first consider the continuity equation:

$$\frac{\partial \rho_i(\boldsymbol{r}, t)}{\partial t} + \nabla \cdot \boldsymbol{J}_i(\boldsymbol{r}, t) = 0. \tag{13}$$

Different contributions to flux are considered :

1. *Diffusive.* Given by Fick's linear response law, under the assumption of steady state. The flux goes from regions of high concentration to lower ones with a magnitude proportional to the gradient,

$$J_i = -D_i \nabla \rho_i,$$

where D_i is the diffusion coefficient or diffusivity. Note that this is a first order approximation since we could as well consider higher (odd) order derivatives.

2. *Conductive.* It can be rewritten in terms of diffusion coefficient due to fluctuation-dissipation by using Einsteins relation:

$$J_i = \rho_i v_i = D_i \frac{z_i e \rho_i E}{k_B T}.$$

v_i refers to the flux velocity and E to the electric field within the system. Velocity is the ratio between the electric force ($z_i e E$) and the Stokesian friction term ($6\pi\eta a_i$, being a_i the ionic radius). Moreover, as usual, $E = -\nabla\psi$.

Therefore, after the mentioned considerations we find out that flux as following form:

$$J_i = D_i(\nabla\rho_i + \frac{z_i e \rho_i}{k_B T} E). \tag{14}$$

Note that this is consistent with the previous derivation since under equilibrium assumption ($J_i = 0$) it is trivial to check that we actually recover the Boltzmann distribution of Eq.(7) for the ionic density.

2.4 Poisson-Nernst-Planck equation

Joining all the concepts presented in Eqs.(6),(13) and (14) we can derive the so called classical Poisson-Nernst-Planck (PNP) equations, in order to model the ionic dynamics, assuming not only spatial but also time dependence. We focus on a planar geometry with normal coordinate z and invariance in the x and y directions and we consider only one specie, unique i, such that we can write the PNP equations as

$$\begin{aligned} \partial_z^2\phi(z,t) &= -\kappa^2 \left[\frac{\rho_+(z,t) - \rho_-(z,t)}{2\rho_b}\right], \\ \partial_t\rho_\pm(z,t) &= -\partial_z j_\pm(z,t), \\ j_\pm(z,t) &= -D\left[\partial_z\rho_\pm(z,t) \pm \rho_\pm(z,t)\partial_z\phi(z,t)\right]. \end{aligned} \tag{15}$$

Recall that, $\boldsymbol{J_\pm(r)\cdot\hat{z} = j_\pm(z)}$, thus, $\boldsymbol{j}_\pm$ describes the ionic flux along z axis. With this set of equations, our main goal now is to set boundary conditions which help us describing our system as accurately as possible.

2.5 Multiple stack model

As a short preview of the proposed model we wish to describe a cathode and an anode, both are of thickness H and with a surface distance $2L$ as shown in Figure.14. In order to mimic the porous structure of the cathode at potential $\Phi(t)$ and the anode at potential $-\Phi(t)$, we defined the planes $Z_i = \pm[L-(i-1)h]$ and set $\phi(\mp Z_i, t) = \pm\Phi(t)$. The porosity is mimicked by $h = \frac{H}{n-1}$ for $n \geq 2$, while the model reduces to the single-plate capacitor for case $n = 1$.

Once the theoretical background is presented it is time to face up with the physical Electrode-Electrolyte system concerning this thesis. First of all, the simplest set up is analyzed in order to get a deeper understating of the problem. Later on, we increase the dimension of the system as a way to introduce matrix notation and to finish with general n problem, which is our final goal.

3 Single-plate capacitor

To begin with, single-plate capacitor case is used to analyse the system under easier conditions, because although it contains the same physics, it is way more manageable and illuminating.

3.1 Step function potential

Analysis of the simplest case with a sudden switching on the potential is presented by using two different approaches, finding analytical solution to the PNP equations and solving the equivalent RC circuit model.

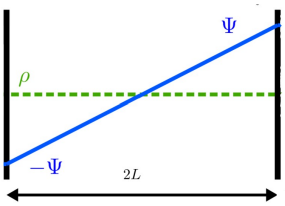

Figure 2: Diagram of our stack electrode model for the case that it reduces to a single-plate capacitor of $2L$ width. Such system is shown at $t = 0$, when potential difference is set to be 2Ψ and ionic densities take value $\rho_{\pm}(z, t = 0) = \rho_b$.

As shown in Fig.2 potential difference is set at the initial time,i.e.:

$$\phi(\pm L, t) = \begin{cases} 0 & t < 0, \\ \mp\Phi_0 & t \geq 0. \end{cases} \tag{16}$$

This sudden switching on of the potential should produce a increase of the surface charge on the electrode's plates until it reaches a saturation value when is it completely charged. This behaviour is qualitatively represented in Fig.3. Its time dependency will vary according to the geometry of the system.

3.1.1 Analytical Solutions

Equations that describe the ionic dynamics of the system described in Figure.2 have already been given in Eq.(15), which under some concrete assumptions can be analytically solved. Boundary conditions, are given by the fact that electrodes have to be impermeable and the voltage difference between both electrodes is $2\Phi_0$, hence

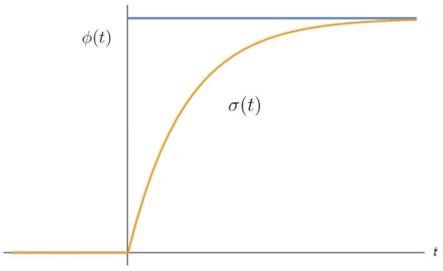

Figure 3: Qualitative illustration of how step function potential causes an increase on the surface charge of the electrodes in the single-plate capacitor.

$$\begin{cases} j_{\pm}(\pm L, t) = 0, \\ \phi(\pm L, t) = \mp\Phi_0. \end{cases} \tag{17}$$

These equations can be actually rewritten in such way that we make variables dimensionless which will simplify the procedure to find out solution which is indeed hard in itself. Let us define relative charge density and relative ion concentration as $\rho_e = \frac{\rho_+ - \rho_-}{2\rho_b}$ and $c = \frac{\rho_+ + \rho_-}{2\rho_b}$. Similarly we make time and position dimensionless $z^* = \frac{z}{L}$ and $\tau = t\frac{\kappa D}{L}$. Relative charge and concentration flux, $j_e = -(\partial_{z^*}\rho_e + c\partial_{z^*}\phi)$ and $j_c = -(\partial_{z^*}c + \rho_e\partial_{z^*}\phi)$. To end up with, let us taking a dimensionless parameter $\lambda = \frac{1}{\kappa L}$.
One remark regarding to notation: *dimensionless physical quantities* such as time or potential will always be noted by using τ and ϕ (or Φ) while other quantities will be marked with the * symbol (λ does not represent any quantity, that is why * is not used). PNP can be rewritten dimensionless as follow:

$$\begin{aligned} \partial_z^2\phi(z^*,\tau) &= -\lambda^{-2}\rho_e(z^*,\tau), \\ \partial_\tau\rho_{e,c}(z^*,\tau) &= -\lambda\partial_{z^*}j_{e,c}(z^*,\tau), \\ j_e(z^*,\tau) &= -(\partial_{z^*}\rho_e(z^*,\tau) + c(z^*,\tau)\partial_{z^*}\phi(z^*,\tau)), \\ j_{e,c}(\pm 1,\tau) &= 0, \\ \phi(\pm 1,\tau) &= \mp\Phi_0. \end{aligned} \tag{18}$$

Under assumption of small potential $\Phi_0 \ll 1$, then $c \approx 1$, since a small potential at the electrodes would make derivatives of potential remain small, hence, j_c will be small in the system. Joining first three equations above the following differential equation is obtained, while boundary conditions are maintained:

$$\frac{\partial\rho_e(z^*,\tau)}{\partial\tau} = \lambda\frac{\partial^2\rho_e(z^*,\tau)}{\partial z^{*2}} - \frac{1}{\lambda}\rho_e(z^*,\tau). \tag{19}$$

By using the methods described in Appendix A.1 in Laplacian space Eq.(19) transforms as

$$s\overline{\rho_e}(z^*,s) - \rho_e(z^*,0) = \lambda\frac{d^2\overline{\rho_e}(z^*,s)}{dz^{*2}} - \frac{1}{\lambda}\overline{\rho_e}(z^*,s). \tag{20}$$

Note that the relative ionic density evaluated in $t = 0$ is null because $\rho_-(z^*,0) = \rho_+(z^*,0)$. Then, Eq.(20) becomes:

$$\frac{d^2\overline{\rho_e}(z^*,s)}{dz^{*2}} = k^2\overline{\rho_e}(z^*,s), \tag{21}$$

where $k^2 = \frac{1}{\lambda^2}(1+s\lambda)$. Solutions are straightforward and applying the fact that we require to be anti symmetric, i.e, $B(s) = 0$, our solution

$$\overline{\rho_e}(z^*,s) = A(s)\sinh kz^*. \tag{22}$$

where $A(s)$ is explicitly shown in Apppendix A.1 since we consider it's not essential for the understanding of the derivation. By now, it is enough to know it's a function of s. Boundary conditions have to be transformed as well to the Laplacian space,

$$\begin{cases} \overline{j_e}(\pm 1,s) & = 0, \\ \overline{\phi}(\pm 1,s) & = \mp\frac{\Phi_0}{s}. \end{cases} \tag{23}$$

Solution for dimensionless charge density in Laplacian space is given by:

$$\overline{\sigma^*}(s) = \frac{2A(s)}{k\lambda}(1-\cosh k). \tag{24}$$

As explained in Appendix A.1, under Debye time, t_D, some neighbour ions might have swapped their position, however, neutrality is maintained because voltage had no time change. In other words,the system shows little reaction for $t_D \gg t$.
Under such condition we get:

$$\overline{\sigma^*}(s) = \frac{K_{\sigma^*}s^{-1}}{1+s\tau_{\sigma^*}}, \tag{25}$$

where K_{σ^*} and τ_{σ^*} terms are explicity shown in Appendix A.1. However, the main point is that inverse for Eq.(25) is indeed straightforward,

$$\sigma^*(\tau) = K_{\sigma^*}(1-e^{-\frac{\tau}{\tau_{\sigma^*}}}). \tag{26}$$

Moreover, if $\kappa^{-1} \ll L$, i.e. , if we assume that width of the capacitor is much bigger than Debye's length, then the dimensionless quantities defined before become more manageable,

$$\tau_{\sigma^*} \approx 1 - \frac{\lambda}{2},$$

$$K_{\sigma^*} \approx \pm 2\Phi_0.$$

Under this assumption dimensionless charge density and the actual relaxation time :

$$\sigma^*(\tau) \approx \pm 2\Phi_0(1-e^{\frac{-\tau}{1-\frac{\lambda}{2}}}), \tag{27}$$

$$t_{relax} \approx \frac{L}{\kappa D}(1-\frac{1}{2\kappa L}). \tag{28}$$

with $t_{RC} = \frac{L}{\kappa D}$. Note that dimensionless time can be actually rewritten as $\tau = t\kappa^2 D\lambda$, where λ is an non-dimensional parameter so that we can plot the Eq.(27) for different values by using $\propto \exp\left[\frac{-t\kappa^2 D}{\frac{1}{\lambda}-\frac{1}{2}}\right]$:

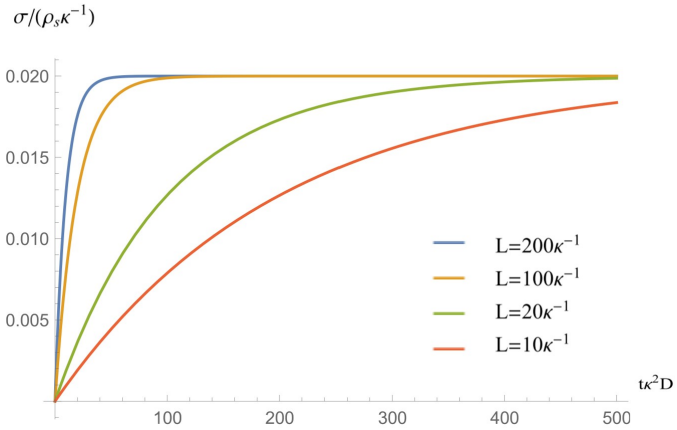

Figure 4: Plot of the analytic result of the surface charge density for small potential, Φ_0=0.01, by using $\lambda^{-1} = 10, 20, 100, 200$ vs the dimensionless time $t\kappa^2 D$.

Figure.4 is replication from [15] with our own code, since we consider it actually shows some interesting futures of the double layer system. The dimensionless parameter λ represents the ratio between the half distance among electrodes and the Debye length. So basically in this plot we can see how fast is the system charged for different values of separations among electrodes. The bigger the separation within the electrodes the faster the charge density reaches the saturation value.

3.1.2 Circuit modelling

We can also model the single-plate capacitor as a RC circuit in order to compare results got from the analytical ones. The EDLs are modeled by a capacitor of C capacitance and electrolyte resistance by resistor of R resistance.

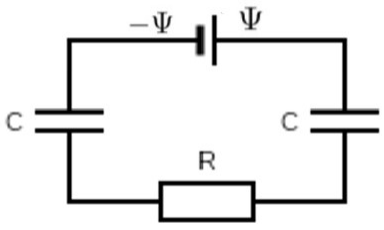

Figure 5: Our proposed equivalent RC circuit model for the simple case in which general system is reduced to a single plate capacitor.

Initially a voltage difference of 2ψ is applied. Therefore, the capacitors, initially uncharged, start to charge by $Q(t) = C\Delta\Psi(t)$, where $\Delta\Psi(t)$ is the time-dependent voltage drop

in the capacitor. By Kirchhoffs Law, the applied voltage difference has to be equal to the drop in all the components of the circuit, which means $2\Psi = 2\Delta\Psi(t) + IR$.
The current flowing through the system can be deduced by the Ohm's law, $I = \dot{Q}(t) = C\Delta\dot{\Psi}(t)$ so we therefore have the differential equation that describes our system with the initial condition of the capacitors being uncharged, i.e.,

$$\Delta\dot{\Psi}(t) = [\Psi - \Delta\Psi(t)]\frac{2}{RC},$$
$$\Delta\Psi(t=0) = 0,$$

which solution is the following:

$$\Delta\Psi(t) = \Psi\left[1 - e^{-\frac{2t}{RC}}\right]. \tag{29}$$

By substituting the solution we are actually able to describe the charge within the capacitor on time,

$$Q(t) = C\Psi\left[1 - e^{-\frac{t}{t_{RC}}}\right], \tag{30}$$

with $C = A\epsilon\kappa$ and $R = \frac{2L}{A\epsilon\kappa^2 D}$. Besides, $t_{RC} = \frac{RC}{2}$ is known as RC time, previously defined as,

$$t_{RC} = \frac{L}{\kappa D}. \tag{31}$$

Eq.(28) is indeed a result of great importance because it shows that the relaxation time of the system is basically equal to RC time when $\kappa L \gg 1$. Thus, we find that surface charge from the analytical solution and charge of the RC circuit equation have the same behaviour. Moreover, we can actually see how RC time depends on the geometry of the system. Current is, thus, obtained:

$$I(t) = \frac{2\Psi}{R}e^{\frac{-t}{t_{RC}}}. \tag{32}$$

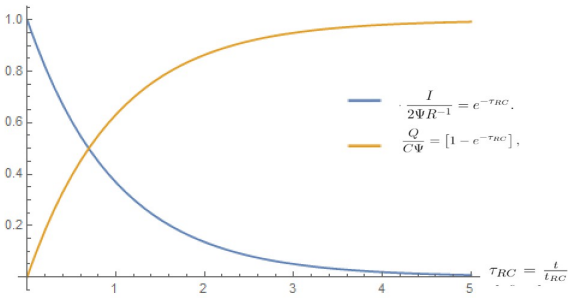

Figure 6: Plot of the time dependence of the dimensionless surface charge (orange) and current (blue) of the single-plate capacitor in our RC circuit model.

3.2 Time dependent potential

Now we would like to analyse the behaviour of the single-plate capacitor in case the applied potential difference varies with time. Thus, we shall consider the case in which the applied potential is not anymore a step function in which the potential remains constant over time but could have any given time dependence. Required equations are already given in Eq.(28), but now slightly modified introducing $\Psi(t)$ since now the voltage is time dependent. The solution to Eq.(28) is fully detailed in the Appendix A.2, obtaining the following expression for the voltage within the capacitors

$$\Delta\Psi(t) = \frac{1}{t_{RC}} e^{-\frac{t}{t_{RC}}} \int_0^t \Psi(t') e^{\frac{t'}{t_{RC}}} dt'. \tag{33}$$

Until this point we basically derived how the potential changes over time in the capacitors under a time dependent potential. We now introduce cyclic voltammetry (CV) [17] which is a powerful technique in the field of electrochemistry. Due to its simplicity, the triangular-shaped potential from Fig.(7) is chosen, which varies linearly with time up to a maximum Ψ_0 at $t = t_0$, after which it decays linearly towards $\Psi(t) = 0$ at $t = 2t_0$. Therefore, we can define $\theta = \frac{\Psi_0}{t_0}$, as the velocity at which the system reaches the fixed maximum potential.

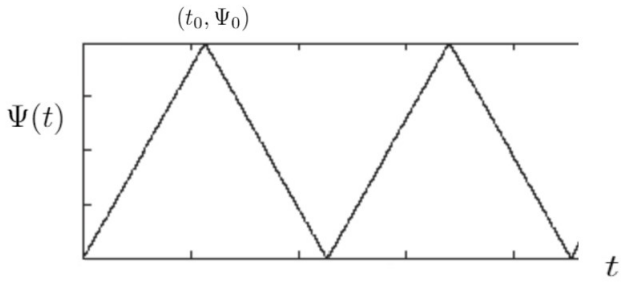

Figure 7: Cualitative plot of the applied triangular shape potential.

This periodic function plotted in Figure.7 can be expanded in Fourier base as follows,

$$\Psi(t) = \Psi_0 \left[\frac{1}{2} - \frac{4}{\pi^2} \sum_{m=1,3,5...}^{\infty} \frac{1}{m^2} \cos\left(\frac{m\pi}{t_0} t \right) \right]. \tag{34}$$

with Ψ_0 the maximum value at which potential in set and t_0^{-1} the scan rate, both are parameters chosen by us. I personally think it is important now to explicitly define non dimensional time scales which will be used in the following sections once and again.

$$\tau_{RC} = \frac{t}{t_{RC}}, \ \tau_0 = \frac{t}{t_0}, \ \alpha = \frac{t_{RC}}{t_0}.$$

where α is the ratio between both time scales, which we might denominate "coupling constant of the circuit". It is important to note that unlike in the case of the sudden switching-on of the potential, we find out that there are two different time-scales now, t_{RC} of the circuit and t_0 of the source term. Once the Fourier transform of the applied potential is known general solution is given by substituting it into Eq.(33),

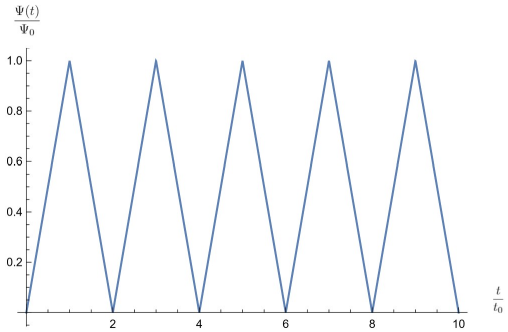

Figure 8: Plot of the applied triangular potential by using Eq.(34) with $m_{max} = 1001$.

$$\Delta\Psi(t) = \frac{\Psi_0}{t_{RC}} e^{-\frac{t}{t_{RC}}} \left[\int_0^t \left[\frac{1}{2} - \frac{4}{\pi^2} \sum_{m=1,3,5...}^{\infty} \frac{1}{m^2} \cos\left(\frac{m\pi}{t_0} t'\right) \right] e^{\frac{t'}{t_{RC}}} dt' \right]. \tag{35}$$

In order to get to full solution we just integrate as it is explained into Appendix A.3, getting the following expression:

$$\Delta\Psi(t) = \Psi_0 \left[\frac{(1 - e^{-\frac{t}{t_{RC}}})}{2} - \frac{4}{\pi^2} \sum_{m}^{\infty} \frac{1}{m^2} \frac{\cos\left(\frac{m\pi}{t_0} t\right) + m\pi\alpha \sin\left(\frac{m\pi}{t_0} t\right) - e^{-\frac{t}{t_{RC}}}}{1 + (m\pi\alpha)^2} \right]. \tag{36}$$

However, we might be interested on how the current changes over time. Therefore computing the derivative of Eq.(36) it is straightforward to get:

$$I(t) = \frac{2\Psi_0}{R} \left[\frac{e^{-\frac{t}{t_{RC}}}}{2} - \frac{4}{\pi^2} \sum_{m}^{\infty} \frac{1}{m^2} \frac{(m\pi\alpha)^2 \cos\left(\frac{m\pi}{t_0} t\right) - (m\pi\alpha) \sin\left(\frac{m\pi}{t_0} t\right) + e^{-\frac{t}{t_{RC}}}}{1 + (m\pi\alpha)^2} \right]. \tag{37}$$

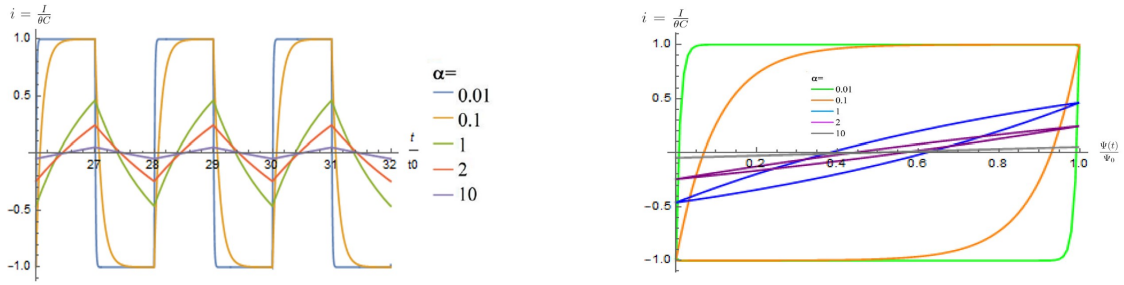

(a) (b)

Figure 9: In Figure (a) Dimensionless current $i = \frac{I}{\theta C}$ plotted vs $\frac{t}{t_0}$ during three periods where $\frac{t}{t_0} \in [26,32]$ (b) Dimensionless current vs dimensionless potential. These plots were done by using $m_{max} = 1001$.

It is important to note that although the most natural dimensionless quantity $i = \frac{I}{\Psi_0 R^{-1}}$ is not actually plotted but it is indeed more interesting to take $i = \frac{I}{\theta C}$, so that for small values of α we get the biggest values of the current.

Figure.9 (a) is plotted in such time range due to the fact that first oscillations do not give the same current amplitudes because time is not large enough to make the exponential vanish and reach stability, i.e. $\frac{t}{t_{RC}} = \frac{t}{t_0}\frac{t_0}{t_{RC}} = \frac{26}{\alpha}$.

$$\frac{t}{t_{RC}} = \begin{cases} 2600 & \alpha = 0.01, \\ 2.6 & \alpha = 10. \end{cases}$$

Since $\frac{t}{t_{RC}} \geq 2.6$, then $e^{-2.6} \approx 0.07$. Therefore, we can indeed conclude that for such time the contribution of the exponential have essentially disappeared and the system is found to be in a steady state. This is rather important in order to plot Figure.9 (b) because the cycles need to be stable to get a well defined shape and show why we called it cyclic voltymmetry.

4 General Electrode-Electrolyte System.

4.1 First approach to matrix notation by example case n=2

We personally consider that before going to the n general case, could be pretty helpful the case $n = 2$, since it concerns almost same physics and mathematics but is by far more manageable. Therefore, RC model is analysed by using the step potential and cyclic voltammetry.

4.1.1 Step function potential

The proposed circuit is the following,

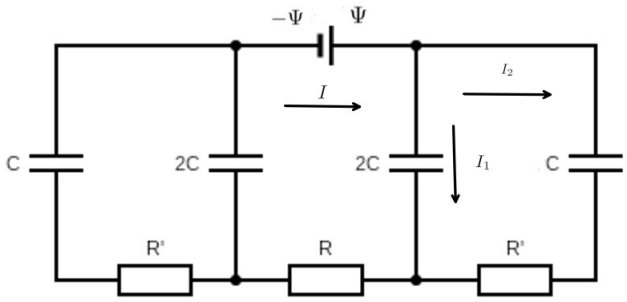

Figure 10: RC circuit for the case $n = 2$

Applying the Kirchhoffs laws, we will end up with the following equations:

$$I = I_1 + I_2,$$
$$2\Psi - 2\Delta\Psi_1(t) - IR = 0,$$
$$-\Delta\Psi_2(t) - I_2R' + \Delta\Psi_1(t) = 0.$$

As in the previous case, current changes with time in capacitors, $I_1(t) = 2C\Delta\dot{\Psi}_1(t)$ and $I_2(t) = C\Delta\dot{\Psi}_2(t)$. Therefore, by simple substitution among the equations describe just above following differential equations are obtained

$$\Delta\dot{\Psi}_1(t) = \frac{\Psi}{RC} - \left(\frac{1}{RC} + \frac{1}{2R'C}\right)\Delta\Psi_1(t) + \frac{1}{2R'C}\Delta\Psi_2(t),$$
$$\Delta\dot{\Psi}_2(t) = \frac{1}{R'C}\Delta\Psi_1(t) - \frac{1}{R'C}\Delta\Psi_2(t),$$

with the following initial conditions:

$$\Delta\Psi_1(t=0) = 0\ ,\ \Delta\Psi_2(t=0) = 0.$$

It is now useful to translate these equations to matrix form since for the general case will be way easier to work with.

$$\begin{pmatrix}\dot{\Delta\Psi_1}(t)\\ \Delta\Psi_2(t)\end{pmatrix} = \frac{\Psi}{RC}\begin{pmatrix}1\\0\end{pmatrix} - \frac{1}{2R'C}\underbrace{\begin{pmatrix}1+2R'/R & -1\\ -2 & 2\end{pmatrix}}_{b}\begin{pmatrix}\Delta\Psi_1(t)\\ \Delta\Psi_2(t)\end{pmatrix}. \tag{38}$$

Eq.(38) can be written as $\dot{X} = A - BX$. One important fact is that matrix B can be diagonalized, since the spectral theorem guarantees that any square matrix with real coefficients is orthogonal diagonalizeable. Hence, we can safely make use of the concepts from basic linear algebra so that B matrix can be rewritten as $B = UDU^{-1}$, being U the normalized matrix with the eigenvectors of B in columns and D the diagonal matrix whose elements are the eigenvalues that correspond to each eigenvector. Since the matrix b is the one being diagonalized we explicity note that $B = \frac{b}{2R'C} = \frac{b}{\frac{2R'}{R}RC} = \frac{b}{2rt_{RC}}$. For this case we can actually try to get fully analytical solutions from which we hopefully can extract some useful information and conclusions. For simplicity we diagonalize the previously mentioned matrix B as a function of the relation between resistors, $r = 2\frac{R'}{R}$. As an important remark regarding to notation Λ_i is used as the non dimensional eigenvalue extracted from the diagonalization of b matrix and λ_i instead for the eigenvalues of matrix B, they are both related as follows:

$$\lambda_i = \frac{\Lambda_i}{2rt_{RC}}.$$

We find the eigenvalues of B, λ_i as and eigenvectors $\boldsymbol{v_i}$ as:

$$\lambda_1 = \frac{3+r+k}{4rt_{RC}} \rightarrow \boldsymbol{v}_1 = \left(\frac{1-r-k}{4}, 1\right),$$

$$\lambda_2 = \frac{3+r-k}{4rt_{RC}} \rightarrow \boldsymbol{v}_2 = \left(\frac{1-r+k}{4}, 1\right),$$

with $k = \sqrt{r^2 - 2r + 9}$, which have been chosen due to the fact that this factors appear once and again in the following derivations. For this specific case the previously mentioned matrices, thus, take the following form:

$$D = \frac{1}{2rt_{RC}}\begin{pmatrix}\Lambda_1 & 0\\ 0 & \Lambda_2\end{pmatrix},\ U = \begin{pmatrix}\frac{1-r-k}{4} & \frac{1-r+k}{4}\\ 1 & 1\end{pmatrix},\ U^{-1} = \begin{pmatrix}-\frac{2}{k} & \frac{k-r+1}{2k}\\ \frac{2}{k} & \frac{k+r-1}{2k}\end{pmatrix},\ A = \frac{\Psi_0}{2t_{RC}}\begin{pmatrix}1\\0\end{pmatrix}.$$

As important remark, eigenvalues in D matrix are sorted by value, being $\Lambda_1 \geq \Lambda_2$.
As we will prove in Section 4.2.3, we can write the general solution to proposed Eq.(58) in the following way:

$$X(t) = U[1 - e^{-Dt}]D^{-1}U^{-1}A. \tag{39}$$

where all matrices are, being $n = 2$ and without lost of generality , the ones defined above. Before stepping into computational simulations I consider it is rather important to extract some information about Eq.(39) in order to verify if it actually describes the system we are looking for. To start with, it can be easily checked that at $t = 0$ the initial condition is indeed fulfilled, $X(t = 0) = 0$. Moreover for large t, as both eigenvalues are positive, we get $X(t \rightarrow \infty) = UD^{-1}U^{-1}A$, which means

$$\frac{X(t\rightarrow\infty)}{\Psi_0} = \frac{2r}{k}\begin{pmatrix}\frac{1-r-k}{4} & \frac{1-r+k}{4}\\ 1 & 1\end{pmatrix}\begin{pmatrix}\frac{1}{\Lambda_1} & 0\\ 0 & \frac{1}{\Lambda_2}\end{pmatrix}\begin{pmatrix}-1\\1\end{pmatrix},$$

if we carry out the matrix multiplication then we end up getting,

$$\frac{X(t\to\infty)}{\Psi_0} = \frac{r}{k}\begin{pmatrix} \frac{4}{3+r-k} - \frac{4}{3+r+k} \\ \frac{1-r+k}{3+r-k} - \frac{1-r-k}{3+r+k} \end{pmatrix}, \tag{40}$$

which shows the fact that for long enough times both capacitors will reach some full charge capacity. Although this expression might look useless at a first glance it will be useful to check if our plot is correct. If the potential is plotted for the simplest possible case analytically speaking, that is to say, $r = 1$. From Eq.(40) we can predict that for large times,

$$\frac{X(t\longrightarrow\infty)}{\Psi_0} = \begin{pmatrix} 1 \\ 1 \end{pmatrix}.$$

Moreover I consider it would be interesting to look for the charge within the capacitors by multiplying with the capacitance $\boldsymbol{Q}(t) = \boldsymbol{C}X(t)$. Thus, the behaviour of the charge is basically the same, with the weighted factor that takes into account different values of the capacitance with the matrix $\boldsymbol{C}$ that represent capacitance so it is a diagonal matrix with weighted values times C.

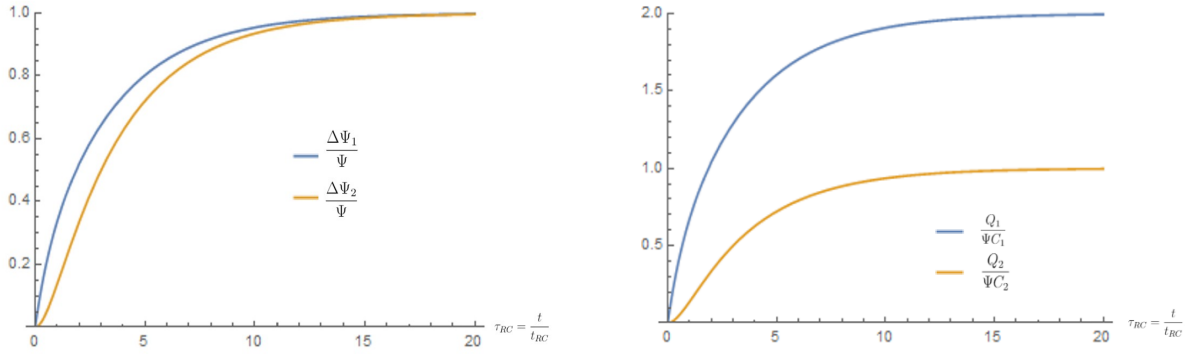

(a) (b)

Figure 11: In plot (a) dimensionless potential $\frac{\Delta\Psi_i}{\Psi}$ vs $\frac{t}{t_{RC}}$, in (b) dimensionless charge $\frac{Q}{\Psi C}$ is plotted vs $\frac{t}{t_{RC}}$ to show the behaviour of the capacitors from the RC circuit model for the example case $n = 2$. Blue line refers to the inner capacitor and orange to the outer one.

In Figure.11(a) we can see that the inner capacitor's, the one related to the biggest eigenvalue, charging process is faster, as expected. Results shown in Figure.11(b) make sense since the capacitance of the outer capacitor is half of the other one doe to the fact that the inner one is twice in contact with the electrolyte.
From Eq.(39) we can derive the current as follows:

$$\boldsymbol{I}(t) = \boldsymbol{C}\dot{X}(t) = \boldsymbol{C}UDe^{-Dt}D^{-1}U^{-1}A. \tag{41}$$

At this point, in order to continue with the simplification of the expression, we think it is important that the reader realized that we can safely take this step, since D and e^{-Dt} are both diagonal matrices, they commute and we can actually exchange their positions getting the following,

$$\boldsymbol{I}(t) = \boldsymbol{C}Ue^{-Dt}U^{-1}\frac{\Psi}{RC}e_1,$$

with $e_1 = (1, 0, ..., 0)$, reduced to $e_1 = (1, 0)$ within this example analysis of case $n = 2$.

$$\boldsymbol{i}(t) = \frac{\boldsymbol{I}(t)}{\Psi R^{-1}} = \begin{pmatrix} 2 & 0 \\ 0 & 1 \end{pmatrix} Ue^{-Dt}U^{-1}e1, \tag{42}$$

this equation although simple, show us an interesting future of the multi-parallel-plate system. When substituting $t = 0$ we get no current in the outer branch of the circuit,

$$\boldsymbol{i}(t=0) = \begin{pmatrix} 2 & 0 \\ 0 & 1 \end{pmatrix} UU^{-1}e1 = \begin{pmatrix} 2 \\ 0 \end{pmatrix}, \tag{43}$$

which means that at early times $t \ll t_{RC}$ the circuit will behave exactly as the simple model one and when times go on then current will start flowing to the outer capacitors. Moreover, when time goes to infinity it is straightforward to check that current goes to 0 in the whole system, because the capacitors charge completely and current cannot flow anymore.
The analytical expression for the current matrix is given by the following equation in terms of r,

$$\boldsymbol{i}(t) = \begin{pmatrix} -\frac{1-r-k}{k}e^{-\frac{\Lambda_1}{2r}\tau_{RC}} + \frac{1-r+k}{k}e^{-\frac{\Lambda_2}{2r}\tau_{RC}} \\ -\frac{2}{k}e^{-\frac{\Lambda_1}{2r}\tau_{RC}} + \frac{2}{k}e^{-\frac{\Lambda_2}{2r}\tau_{RC}} \end{pmatrix}, \tag{44}$$

For the case $r = 1$ then $k = 2\sqrt{2}$ this matrix reduces to:

$$\boldsymbol{i}(t) = \begin{pmatrix} e^{-\frac{2-\sqrt{2}}{2}\tau_{RC}} + e^{-\frac{2+\sqrt{2}}{2}\tau_{RC}} \\ \frac{1}{\sqrt{2}}\left[e^{-\frac{2-\sqrt{2}}{2}\tau_{RC}} - e^{-\frac{2+\sqrt{2}}{2}\tau_{RC}}\right] \end{pmatrix}, \tag{45}$$

Eq.(45) is plotted to indeed check that our predictions made just with basic algebra are completely fulfilled.

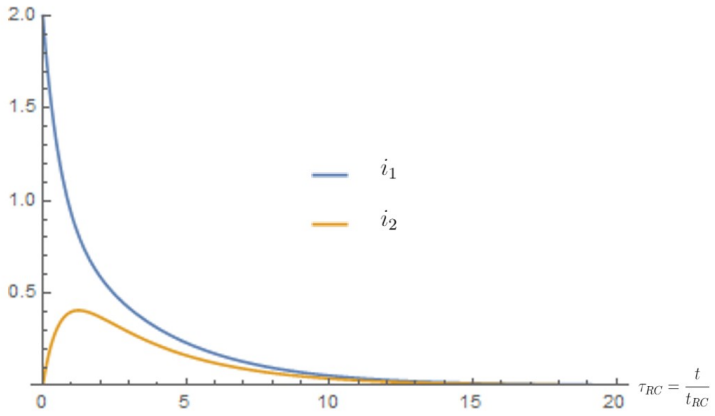

Figure 12: Dimensionless currents $i = \frac{I}{\Psi R^{-1}}$ plotted for RC time scale, solution of the RC circuit model for the example case $n = 2$

Although getting the exact form for the current in the case $n = 2$ does not seem something really useful, due to the fact that this could be easily calculated just by multiplying the matrices using the computer, we personally think it's rather interesting to see how exponential of different eigenvalues are linearly combined for each of the currents in the circuit model. Since this is the only case we consider it's doable and gives us some basic knowledge of how things work before enter into general case.

4.1.2 Time-dependent potential

For the time dependent potential case with $n = 2$, we just consider slight change into the A matrix so that the potential within it is no more constant, therefore we are now considering $A(t)$. As done before general solution is presented which will later be largely discussed. Here we will just focus on the final expression for the solution $X(t)$ of Eq.(63) given by:

$$X(t) = \frac{\Psi_0}{2t_{RC}} U \int_0^t \frac{\psi(s)}{\Psi_0} e^{D(s-t)} ds \; U^{-1} e_1. \tag{46}$$

Eq.(46) is basically equivalent to Eq.(35) valid for any chosen form of $\psi(t)$. As before, we will make use of the triangular potential plotted in Fig.7 which makes our lives easier since the integral has already been solved in Appendix A.3. Solution is presented in an compact way:

$$X(t) = \frac{\Psi_0}{2t_{RC}} U \begin{pmatrix} \Omega_{11} & 0 \\ 0 & \Omega_{22} \end{pmatrix} U^{-1} e_1, \tag{47}$$

where $\Omega_{ii}(t) = \frac{1}{\lambda_i}\left[\frac{(1-e^{-\lambda_i t})}{2} - \frac{4}{\pi^2}\sum_m^\infty \frac{1}{m^2} \frac{\cos\left(\frac{m\pi}{t_0}t\right) + (\frac{m\pi}{t_0\lambda_i})\sin\left(\frac{m\pi}{t_0}t\right) - e^{-\lambda_i t}}{1+(\frac{m\pi}{t_0\lambda_i})^2}\right]$ are the results of the integration of the potential. Remaining matrices above have already been defined for the case $n = 2$ in section 4.1.1. We find important, however, to note that the matrix $\boldsymbol{\Omega_i}$ has time-dimension due to the fact that we have the eigenvalue's inverse as pre-factor.
As done for the step potential case, the next steps will be towards getting the analytical solutions. Reducing the general problem to $n = 2$ case we end up getting

$$X(t) = \frac{\Psi_0}{4kt_{RC}} \begin{pmatrix} -\Omega_{11}(1-r-k) + \Omega_{22}(1-r+k) \\ 4(-\Omega_{11} + \Omega_{22}) \end{pmatrix}, \tag{48}$$

which for the case analysed before, $r = 1$:

$$\frac{\boldsymbol{X}(t)}{\Psi_0} = \frac{1}{4t_{RC}} \begin{pmatrix} \Omega_{11} + \Omega_{22} \\ \sqrt{2}(\Omega_{22} - \Omega_{11}) \end{pmatrix}. \tag{49}$$

The derivative of the elements is given by,

$$\dot{\Omega}_i(\tau_0) = \left[e^{-\frac{\Lambda_i}{2r}\frac{\tau_0}{\alpha}} - \frac{8}{\pi^2}\sum_m^\infty \frac{1}{m^2} \frac{(\frac{2m\pi\alpha r}{\Lambda_i})^2 \cos(m\pi\tau_0) - \frac{2m\pi\alpha r}{\Lambda_i}\sin(m\pi\tau_0) + e^{-\frac{\Lambda_i}{2r}\frac{\tau_0}{\alpha}}}{1 + (\frac{2m\pi\alpha r}{\Lambda_i})^2} \right].$$

Knowing this, it is indeed interesting to look how the current changes in time by just computing the derivative,

$$\boldsymbol{i}(t) = \frac{\boldsymbol{I}(t)}{\Psi_0 R^{-1}} = \frac{1}{4k}\begin{pmatrix} 2 & 0 \\ 0 & 1 \end{pmatrix}\begin{pmatrix} \dot{\Omega}_{22}(1-r+k) - \dot{\Omega}_{11}(1-r-k) \\ 4(\dot{\Omega}_{22} - \dot{\Omega}_{11}) \end{pmatrix}. \tag{50}$$

It is possible to check that current is null at $t = 0$, as expected, knowing the following relation:

$$\sum_{m=0}^{\infty} \frac{1}{(2m+1)^2} = \frac{\pi^2}{8}.$$

Regarding to the general solution it could be interesting to go through the easiest case again where $r = 1$, i.e., $2R' = R$. Under this condition $k = 2\sqrt{2}$ and Eq.(50) becomes,

$$\boldsymbol{i}(t) = \frac{1}{2}\begin{pmatrix} \dot{\Omega}_{11} + \dot{\Omega}_{22} \\ \frac{1}{\sqrt{2}}[\dot{\Omega}_{22} - \dot{\Omega}_{11}] \end{pmatrix}. \tag{51}$$

Similarly to Eq.(45) we have explicitly shown how the matrix elements of Ω are linearly combined to describe the current.

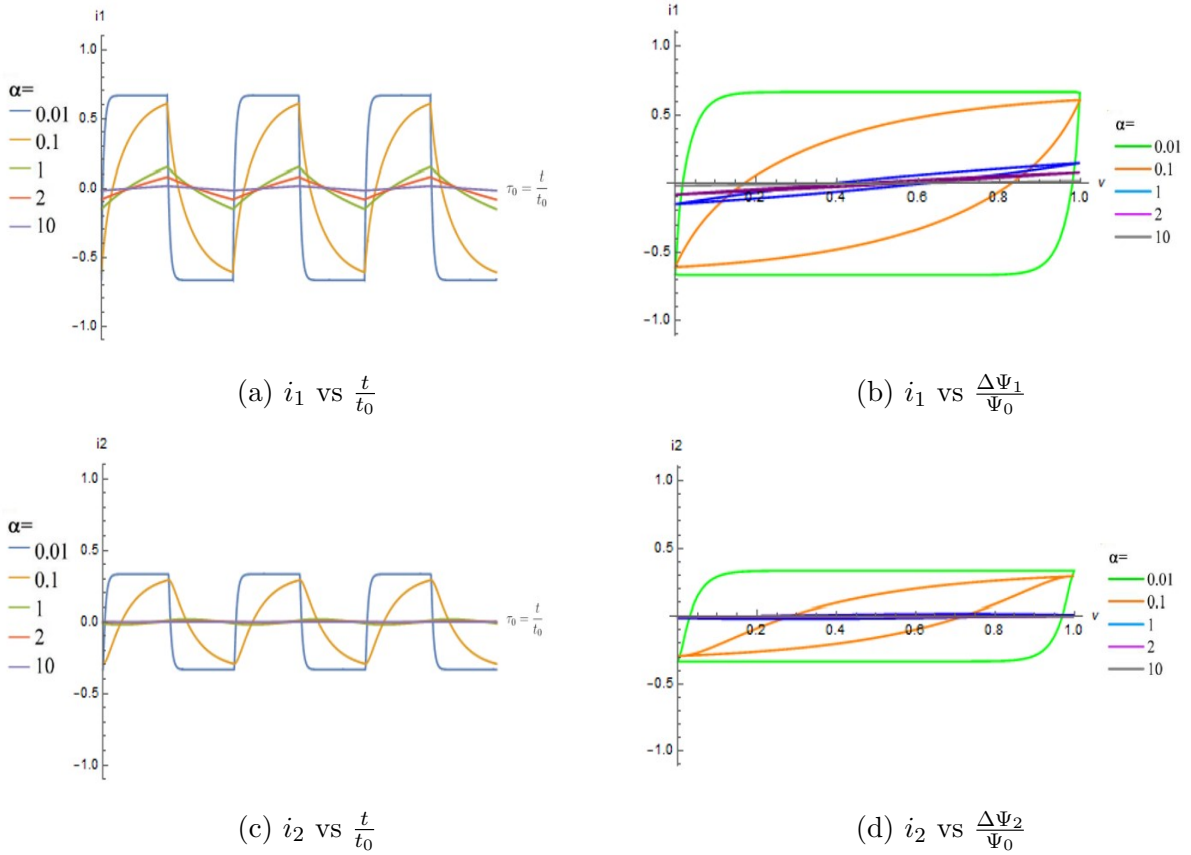

(a) i_1 vs $\frac{t}{t_0}$ (b) i_1 vs $\frac{\Delta\Psi_1}{\Psi_0}$

(c) i_2 vs $\frac{t}{t_0}$ (d) i_2 vs $\frac{\Delta\Psi_2}{\Psi_0}$

Figure 13: Dimensionless current $\frac{I}{3\theta C}$ plotted in time units of $\frac{t}{t_0}$ using in Figures (a), (c) and vs dimensionless potential in (b),(d) by using $m_{max} = 1001$. Each color represents one current for one specific value of α as shown in the color label.

The current, I, through the resistor R, is given by the sum of both currents I_1 and I_2.

4.2 General case

So far we have analysed two concrete cases, $n = 1$, in which general system was reduced to single-plate capacitor and $n = 2$ as a first approach to the matrix problem. Hence, we now need to go one step further considering n electrodes case, as shown in Figure.14.
Porous carbon supercapacitor are now modeled by n equidistant (h) electrodes such that whole thickness of the capacitor equals $H = (n-1)h$. For convenience we shall choose a coordinate system in which $z = 0$ lies in the centre of the capacitor so that $Z_i = \pm(L-(i-1)h)$ where index $i = 1, ..., n$. Moreover, all plates but the outer ones, are permeable to mimic porosity and those ones are made impermeable in order to close the system.

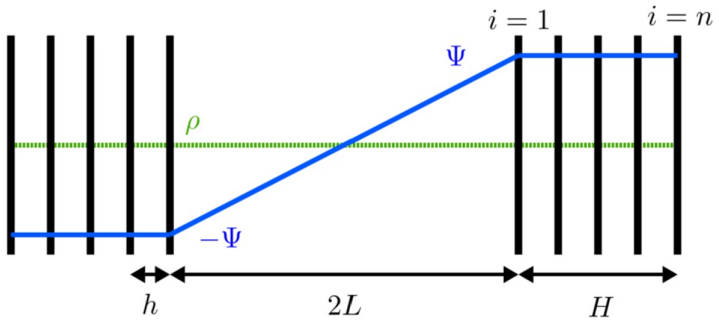

Figure 14: n parallel plates electrode model

4.2.1 Analytical solutions using step- potential

In order to get the general analytical solutions we can actually re use the set of equations used in Section 2.1 since they are still valid.

$$\partial_z^2\phi(z^*,\tau) = -\frac{\rho_e(z^*,\tau)}{\lambda^2},$$
$$\partial_\tau\rho_{e,c}(z^*,\tau) = -\lambda\partial_{z^*}j_{e,c}(z^*,\tau),$$
$$j_e(z^*,\tau) = -(\partial_{z^*}\rho_e(z^*,\tau) + c(z^*,\tau)\partial_{z^*}\phi(z^*,\tau)),$$
$$j_c(z^*,\tau) = -(\partial_{z^*}c(z^*,\tau) + \rho_e(z^*,\tau)\partial_{z^*}\phi(z^*,\tau)),$$

what has to be changed are to boundary conditions since now $2n$ are required:

$$j_{e,c}[\pm(1+(n-1)\frac{h}{L},\tau] = 0,$$
$$\phi[\pm(1+i\frac{h}{L},\tau)] = \mp\Phi_0,$$

In this case we consider it's no more helpful to follow all the steps to reach the solution since we found way more clarifying the simple case and this is just an extension. Therefore we will present the solution given by [15]:

$$\sigma_n^*(\tau) = K_{n,\sigma^*}(1-e^{-\frac{\tau}{\tau_n}}). \tag{52}$$

For $h > 10\kappa^{-1}$ then the approximation made in Section 2.1 is still valid,thus, $K_{n,\sigma^*} = 2\Phi_0$. Now I would like to discuss two different values of $\tau_n = \frac{t_n}{t_{RC}}$. First one is presented in [15] as:

$$\tau_i^n = 2n - 1 - \frac{\lambda}{2} + \frac{h}{L}\sum_{k=0}^{i-2} 2(n-k) - 3, \tag{53}$$

which we found it could actually be simplified as:

$$\tau_i^n = 2n - 1 - \frac{\lambda}{2} + r(i-2)(2n-2-i), \tag{54}$$

where $r = \frac{h}{L}$ in order to be consistent with the notation of the RC model.

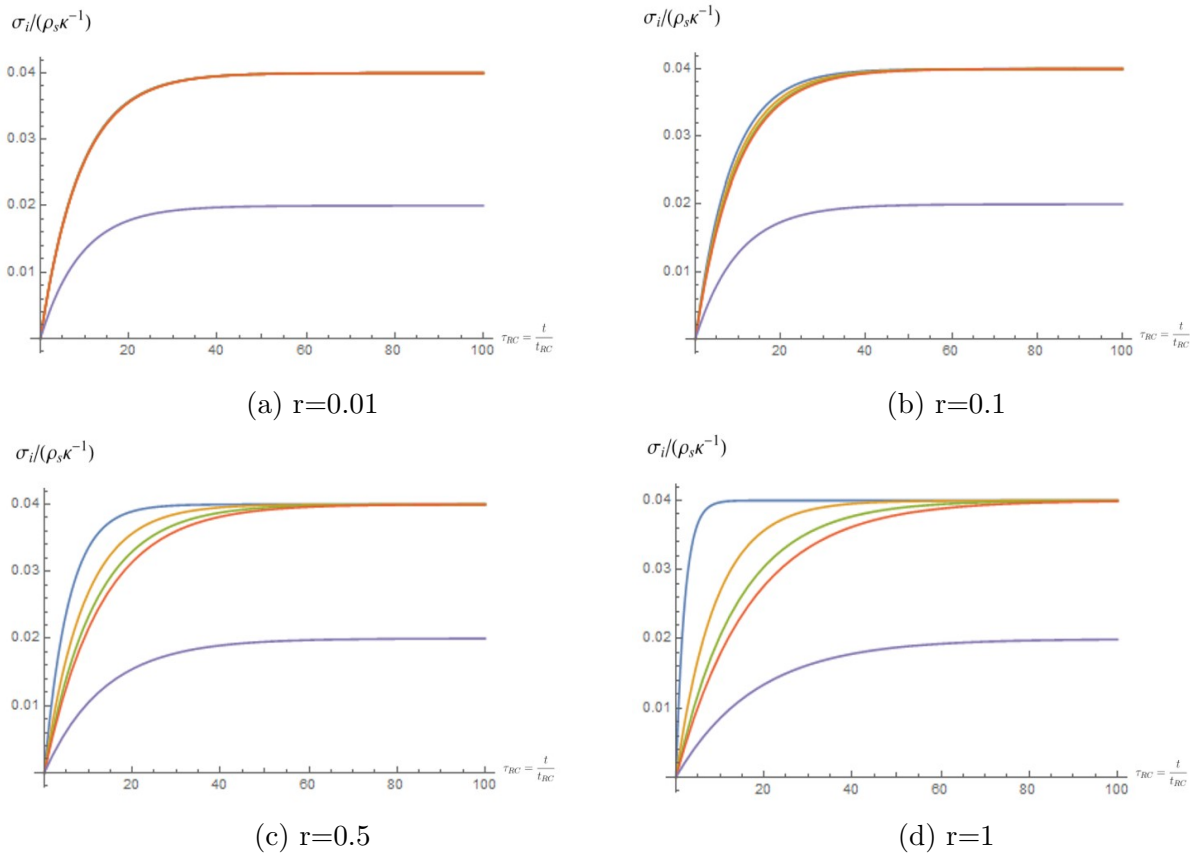

(a) r=0.01

(b) r=0.1

(c) r=0.5

(d) r=1

Figure 15: Dimensionless surface charge plotted vs $\frac{t}{t_{RC}}$ using Eq.(52) and Eq.(54) for $\Phi_0 = 0.01$ and $\lambda = 0.01$ being $n = 5$. As usual, blue line goes for the inner capacitor and last one, purple, for the outer one.

For different values of λ there is no major change in the shape of plots, therefore we consider they do not add more information. Besides when taking the limit of the simple case, this expression reduces to the one found in Section 3.1.1, $\tau_\sigma^* = 1 - \frac{\lambda}{2}$ as it should. Another interesting future is that for very large n we can approximate τ_n^n as:

$$\tau_n^n \approx 2n + r(n^2 - 2n) \tag{55}$$

On the other hand there is another time scale proposed in [13], which have been created by fitting available data. However, it does just describe the relaxation time for the nth capacitor, due to the fact that relaxation rate is dominated by the smallest eigenvalue, which corresponds to the last capacitor.

$$\tau^n = 2n - 1 + r(n-1)(0.75n - 0.91). \tag{56}$$

Eq.(56) correctly reduces to $\tau = 1$ for $n = 1$, for which $\frac{H}{L} = 0$, getting the same result as in Eq.(54) for small values of λ. Besides for large values of n we can actually compare both expression since Eq.(56) can be approximated as follows,

$$\tau^n \approx 2n + r(0.75n^2 - 0.91n). \tag{57}$$

This is rather interesting since for future applications we might be interested in very large values of n, therefore this expressions might give us some insight about it.

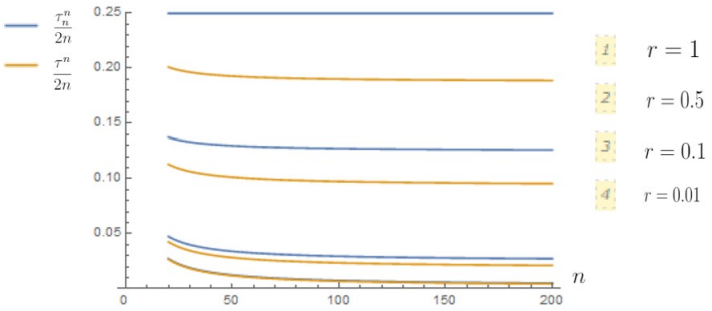

Figure 16: Plot of the two different time scales proposed above. $\frac{\tau_n^n}{2n}$ refers to Eq.(54) and $\frac{\tau^n}{2n}$ Eq.(56) using $r = 1, 0.5, 0.1, 0.01$ for $n \in [20, 200]$.

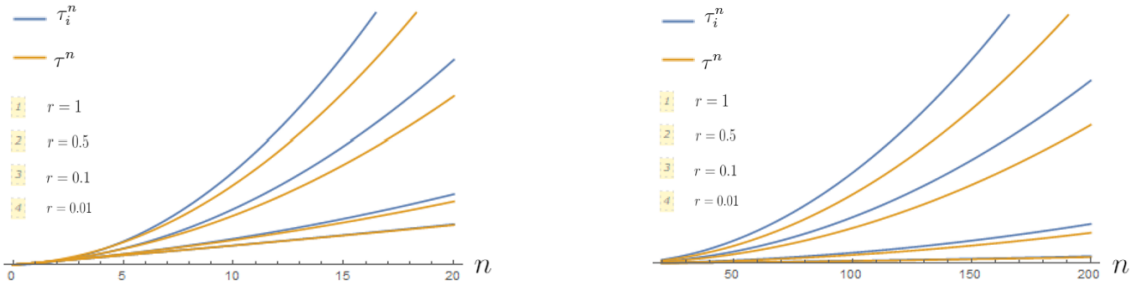

(a) (b)

Figure 17: Plot of the two different time scales, τ_n^n refers to Eq.(54) and τ^n Eq.(56) using r =1,0.5,0.1,0.01.Plot (a) shows for small and (b) for big n.

Results plotted in Figure.17 and .18 could be expected since the difference between them are subjected to the term multipliying $\frac{h}{L}$. Moreover we see that τ_n is large when n is large which suggests that the large relaxation time of super capacitors stems from their large internal surface area achieved though many small pores.

4.2.2 Circuit modelling for the step potential

For the RC general case we actually take into account the fact that the inner electrodes are facing electrolyte twice while the outer ones just once, by the setting capacitances as $2C$ and C respectively.

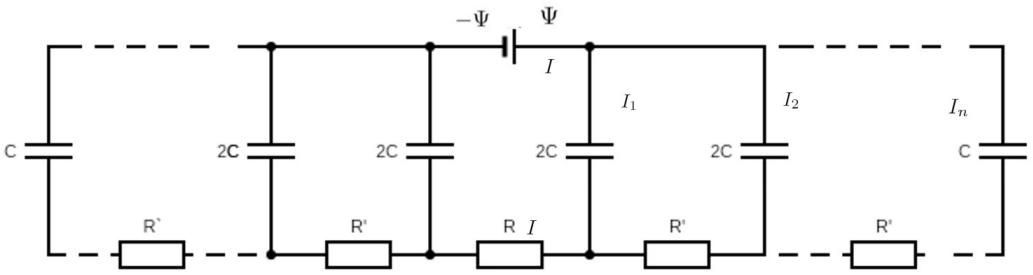

Figure 18: Equivalent RC circuit for the general case

For this case, exactly same principles are applied but we are dealing with a set of n equations. This generalization is presented based on the case $n = 2$ which is way more clarifying and therefore we can straightly present the matricial equation,

$$\begin{pmatrix} \dot{\Delta\Psi_1}(t) \\ \Delta\Psi_2(t) \\ \Delta\Psi_3(t) \\ \vdots \\ \Delta\Psi_n(t) \end{pmatrix} = \frac{\Psi}{RC} \begin{pmatrix} 1 \\ 0 \\ . \\ . \\ 0 \end{pmatrix} - \frac{1}{\frac{2R'}{R}RC} \begin{pmatrix} 1+\frac{H}{L(n-1)} & -1 & & & & \\ -1 & 2 & -1 & & & \\ & -1 & \ddots & \ddots & & \\ & & \ddots & \ddots & -1 & \\ & & & -1 & 2 & -1 \\ & & & & -2 & 2 \end{pmatrix} \begin{pmatrix} \Delta\Psi_1(t) \\ \Delta\Psi_2(t) \\ \Delta\Psi_3(t) \\ \vdots \\ \Delta\Psi_n(t) \end{pmatrix}, \quad (58)$$

note that, in this case, for the top left element we used $H = h(n-1)$ to rewrite $r = 2R'/R = h/L = H/L(n-1)$ hence, $1+r = 1+H/[L(n-1)]$. Furthermore, as done for $n = 2$, Eq.(58) can be written simplified as $\dot{X} = A - BX$, where B is a tridiagonal matrix.

We usually consider writing long derivations on the Appendix, however for this particular case, we think it is worth to explain it within the main text because it is not a long derivation and we consider it rather important. Our aim is to solve the differential equation given in Eq.(58). For doing so, we shall use the matrix decomposition of B explained in section 4.1.1:

$$U^{-1}\dot{X}(t) = U^{-1}A - DU^{-1}X(t)$$

taking $Y(t) = U^{-1}X(t)$ and $A'(t) = U^{-1}A$

$$\dot{Y}(t) = A' - DY(t), \quad (59)$$

basically is solved by integrating each element of the matrix equation ,

$$\int_{Y_i(0)}^{Y_i(t)} \frac{dY_i}{A'_i - \lambda_i Y_i} = \int_0^t dt,$$

being the initial condition $X_i(t=0)=0$, then $Y_i(t=0)=0$

$$ln[A_i' - \lambda_i Y_i]\Big|_0^{Y_i(t)} = -\lambda_i t$$

$$\lambda_i Y_i(t) = (1 - e^{-\lambda_i t})A_i',$$

thus,

$$DY(t) = (1 - e^{-Dt})A'$$

$$UY(t) = U(1 - e^{-Dt})D^{-1}U^{-1}A$$

which finally leads to the general solution already mentioned,

$$X(t) = U[1 - e^{-Dt}]D^{-1}U^{-1}A, \tag{60}$$

Charge is then given by,

$$\boldsymbol{Q}(t) = \Psi_0 \boldsymbol{C} U[1 - e^{-Dt}]\frac{D^{-1}}{2t_{RC}}U^{-1}e_1, \tag{61}$$

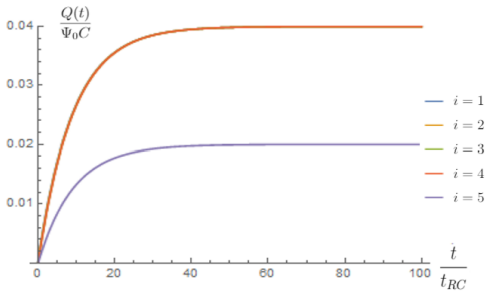

(a) r=0.01

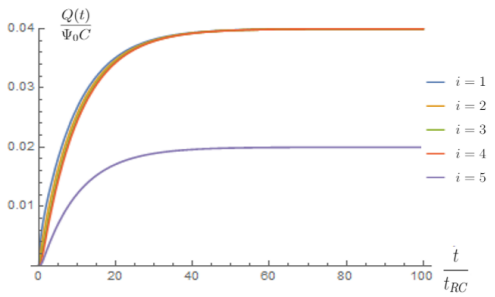

(b) r=0.1

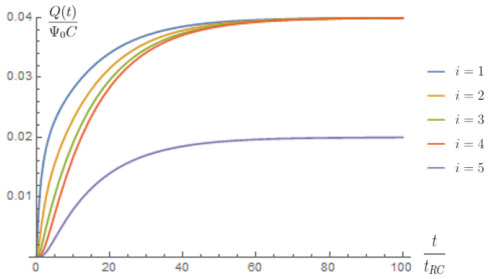

(c) r=0.5

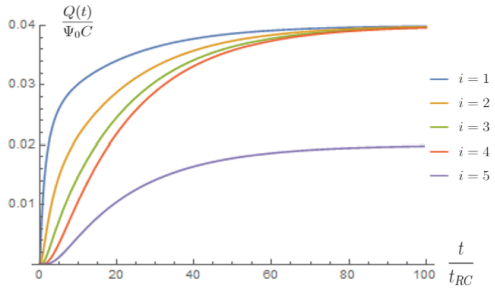

(d) r=1

Figure 19: Dimensionless charge $\frac{Q}{\Psi_0 C}$ vs $\frac{t}{t_{RC}}$ using the solution of the RC circuit being n=5 for different values of r weighted by a factor of $\frac{1}{50}$ which allows us to make a comparison with Figure.15.

The current can be written as:

$$\boldsymbol{i}(t) = \begin{pmatrix} 2 & & & & \\ & 2 & & & \\ & & \ddots & & \\ & & & 2 & \\ & & & & 1 \end{pmatrix} U e^{-Dt} U^{-1} e1, \tag{62}$$

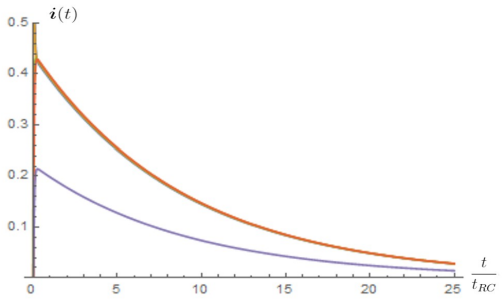

(a) r=0.01

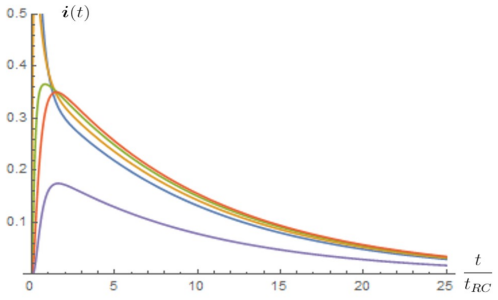

(b) r=0.1

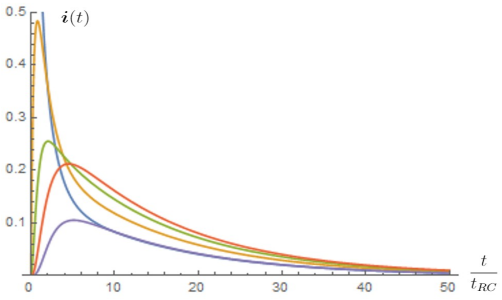

(c) r=0.5

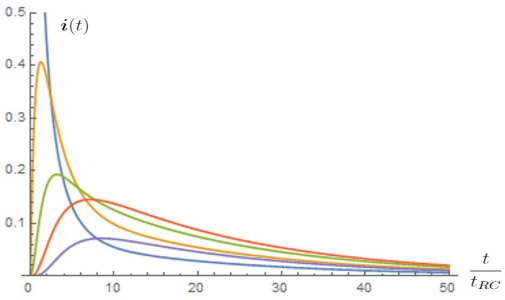

(d) r=1

Figure 20: Dimensionless current $\frac{I}{\Psi R^{-1}}$ vs $\frac{t}{t_{RC}}$ using the solution of the RC circuit being n=5 for a step function potential with different values of r. Blue line gives $i_1(t=0) = 2$ but the scale in y axes is changed in order to have a more detailed vision of how currents change over time. Legends follow the same order as Figure.19.

4.2.3 Circuit modelling for the time-dependent potential

As mentioned for the case $n = 2$ example the general time dependent case can be analysed by solving the following differential equation:

$$\dot{X}(t) = A(t) - BX(t), \tag{63}$$

In order to solve the time dependent potential case we shall begin with Eq.(59) which should be slightly modified in order to be correct since now we are considering $A(t)$,

$$\dot{Y}_i(t) = A_i'(t) - \lambda_i Y_i(t),$$

as before we can integrate the equation in all its i coefficients making use of the method developed for the simple case in the Appendix,

$$Y_i(t) = e^{-\lambda_i t} \int_0^t e^{\lambda_i s} A_i'(s) ds. \tag{64}$$

which is equal to :

$$X(t) = U e^{-Dt} \int_0^t e^{Ds} U^{-1} A(s) ds. \tag{65}$$

Substituting the expression of $A(t) = \frac{\psi(t)}{2t_{RC}} e_1$,

$$X(t) = \frac{\Psi_0}{2t_{RC}} U \int_0^t \frac{\psi(s)}{\Psi_0} e^{D(s-t)} ds \; U^{-1} e_1. \tag{66}$$

where Ω_n is computed as the integral over all the elements in the diagonal matrix

$$\int_0^t \frac{\psi(s)}{\Psi_0} e^{D(s-t)} ds = \begin{pmatrix} e^{-t\lambda_1} \int_0^t \frac{\psi(s)}{\Psi_0} e^{s\lambda_1} ds & & \\ & \ddots & \\ & & e^{-t\lambda_n} \int_0^t \frac{\psi(s)}{\Psi_0} e^{s\lambda_n} ds \end{pmatrix} = \mathbf{\Omega}_n(t) \tag{67}$$

therefore we can once again write the general solution in a more elegant way by:

$$X(t) = \frac{\Psi_0}{2t_{RC}} U \mathbf{\Omega}_n U^{-1} e_1. \tag{68}$$

It's now straightforward to derive both, charge and current as done before,

$$\frac{\boldsymbol{Q}(t)}{C\Psi_0} = \begin{pmatrix} 2 & & & & \\ & 2 & & & \\ & & \ddots & & \\ & & & 2 & \\ & & & & 1 \end{pmatrix} U \frac{\mathbf{\Omega}_n}{2t_{RC}} U^{-1} e_1. \tag{69}$$

with $\frac{\mathbf{\Omega}_i(t)}{2t_{RC}} = \frac{r}{\Lambda_i} \left[\frac{(1-e^{-\lambda_i t})}{2} - \frac{4}{\pi^2} \sum_m^\infty \frac{1}{m^2} \frac{\cos\left(\frac{m\pi}{t_0} t\right) + (\frac{m\pi}{t_0 \lambda_i}) \sin\left(\frac{m\pi}{t_0} t\right) - e^{-\lambda_i t}}{1 + (\frac{m\pi}{t_0 \lambda_i})^2} \right]$ a dimensionless quantity as well. Thus, current is given by:

$$i(t) = \frac{I(t)}{\Psi_0 R^{-1}} = \begin{pmatrix} 2 & & & & \\ & 2 & & & \\ & & \ddots & & \\ & & & 2 & \\ & & & & 1 \end{pmatrix} U\dot{\mathbf{\Omega}}_n U^{-1} e_1, \tag{70}$$

where $\dot{\mathbf{\Omega}}_i(\tau_0) = \frac{e^{-\frac{\Lambda_i}{2r}\frac{\tau_0}{\alpha}}}{2} - \frac{4}{\pi^2}\sum_m^\infty \frac{1}{m^2} \frac{(\frac{2m\pi\alpha r}{\Lambda_i})^2 \cos(m\pi\tau_0) - \frac{2m\pi\alpha r}{\Lambda_i}\sin(m\pi\tau_0) + e^{-\frac{\Lambda_i}{2r}\frac{\tau_0}{\alpha}}}{1+(\frac{2m\pi\alpha r}{\Lambda_i})^2}$. Which I is actually the same as above's expression derivative but we think it is now convenient to rewrite it in terms of τ_0 and α explicitly. Within the case analysed before, i.e., $r = 1$, let us first go with next case $n = 3$:

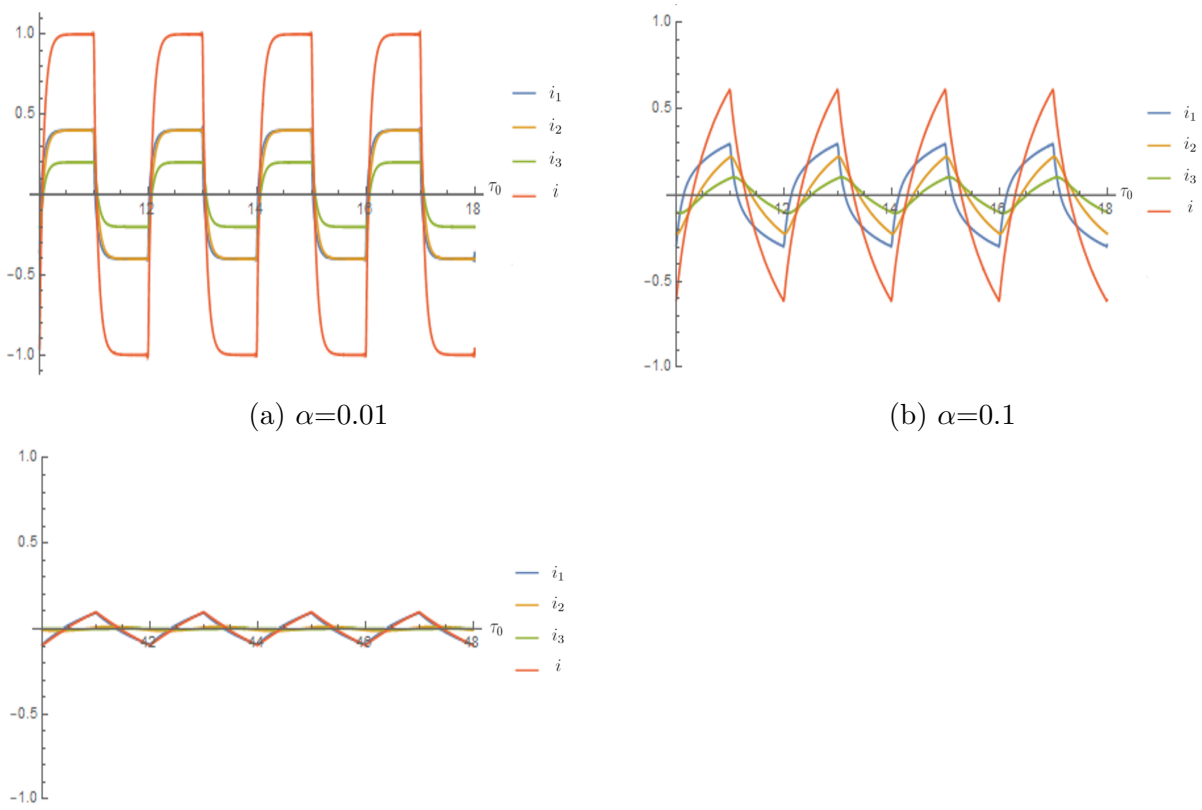

(a) α=0.01

(b) α=0.1

(c) α=1

Figure 21: Dimensionless current $\frac{I}{5\theta C}$ vs $\frac{t}{t_0}$ using the solution of the RC circuit being n=3 for $r = 1$ with $m_{max} = 101$. No more values of α are shown since the amplitude gets so small we consider they do not add any useful information for the reader. i refers to the sum of all the currents

For this chosen case, $r = 1$, we can go up to case $n = 10$. Before presenting it we had to make some adjustments to plots in order to make them more meaningful. For instance, $\sum_k^n i_k$ is not included due to the fact it would not be able to distinguish any differences among the rest of the currents.

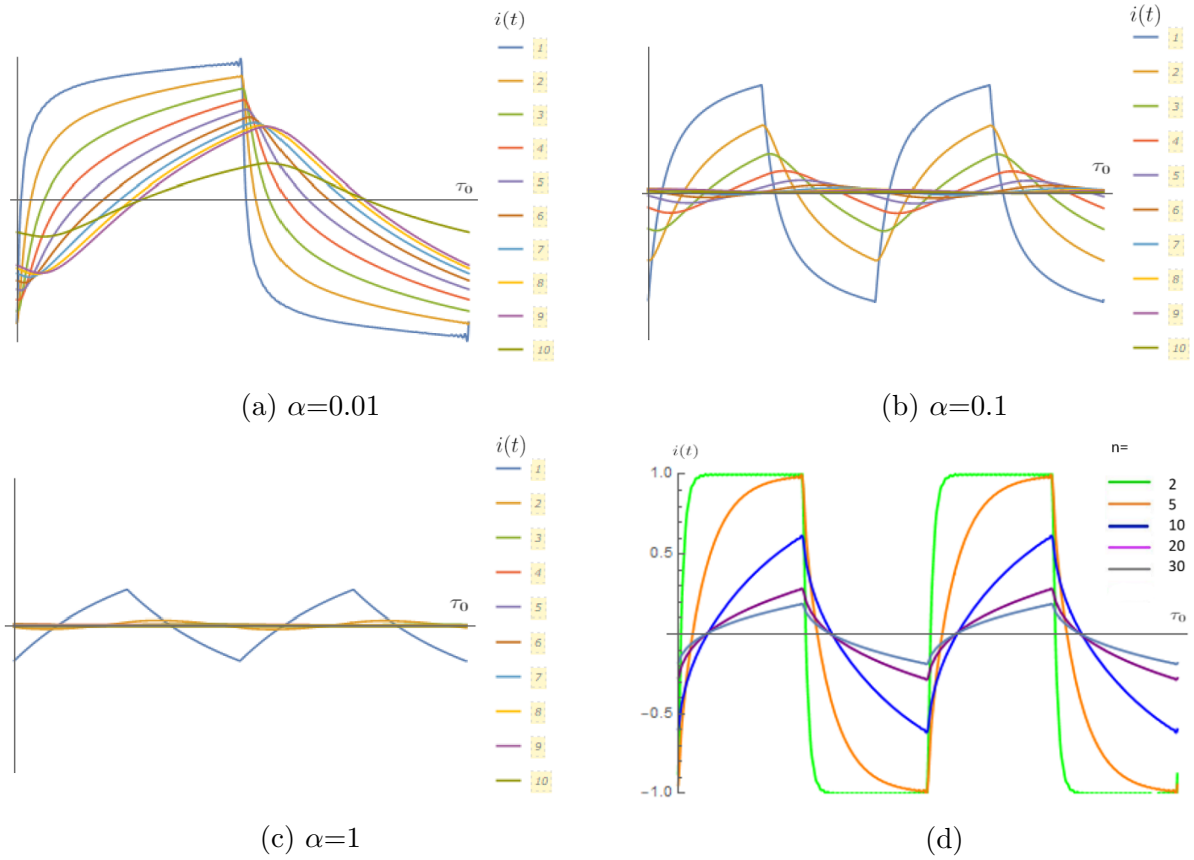

(a) α=0.01 (b) α=0.1

(c) α=1 (d)

Figure 22: In plots (a),(b),(c) $\frac{I}{19\theta C}$ vs $\frac{t}{t_0}$ using the solution of the RC circuit being $n = 10$ for $r = 1$ with $m_{max} = 101$. Values of axes are removed because we want the reader to have a qualitative understanding of the figures. In plot (d) two periods for $\frac{I}{(2n-1)\theta C}$ throughout the R resistor for different values of n being $m_{max} = 51$ and $r = 1$.

Once charging dynamics have been presented we think it is interesting to show some algebraic features about the system extracted from matrix b from Eq.(58) giving our own interpretation related to the system,

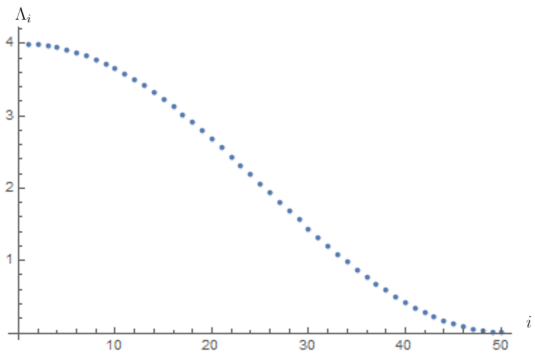

Figure 23: Plot of the distribution of the eigenvalues of b matrix within a system with $n = 50$ and $r = 1$. The sum over all them, $\sum_i^n \Lambda_i = 2n$.

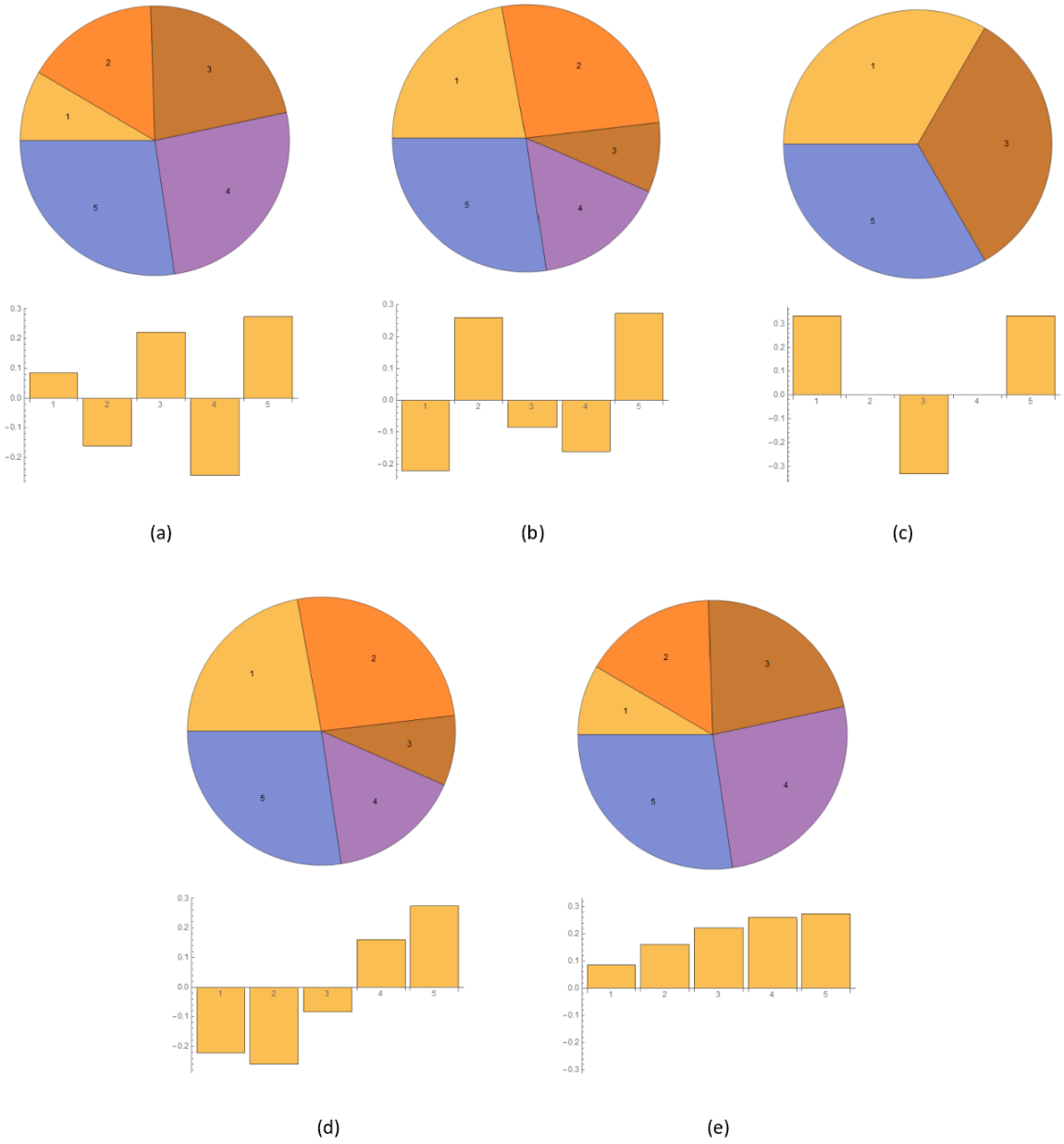

Figure 24: Visual illustration of the eigenvectors of matrix b, taken from the columns of matrix U, for a system with $n = 5$. Each chart represents an eigenvalues, from (a) $\boldsymbol{v}_1$ to (e) $\boldsymbol{v}_5$, shown as a combination of weight-factors related to the currents that go through the branches of the circuit.

In Figure.24 there is a clear symmetry regarding to the contribution of weight-factors associated to currents for each eigenvector with a common feature, the blue chart is always the biggest one, which, if our interpretation is correct must be related to the first current. Besides, it might be even more interesting to reverse it and have a look how eigenvectors affect to the weights of each exponential of the eigenvalue. It might be helpful for the reader to have a glance to Eqs.(44),(45) in order to have a more clear perspective of the refered

situation,

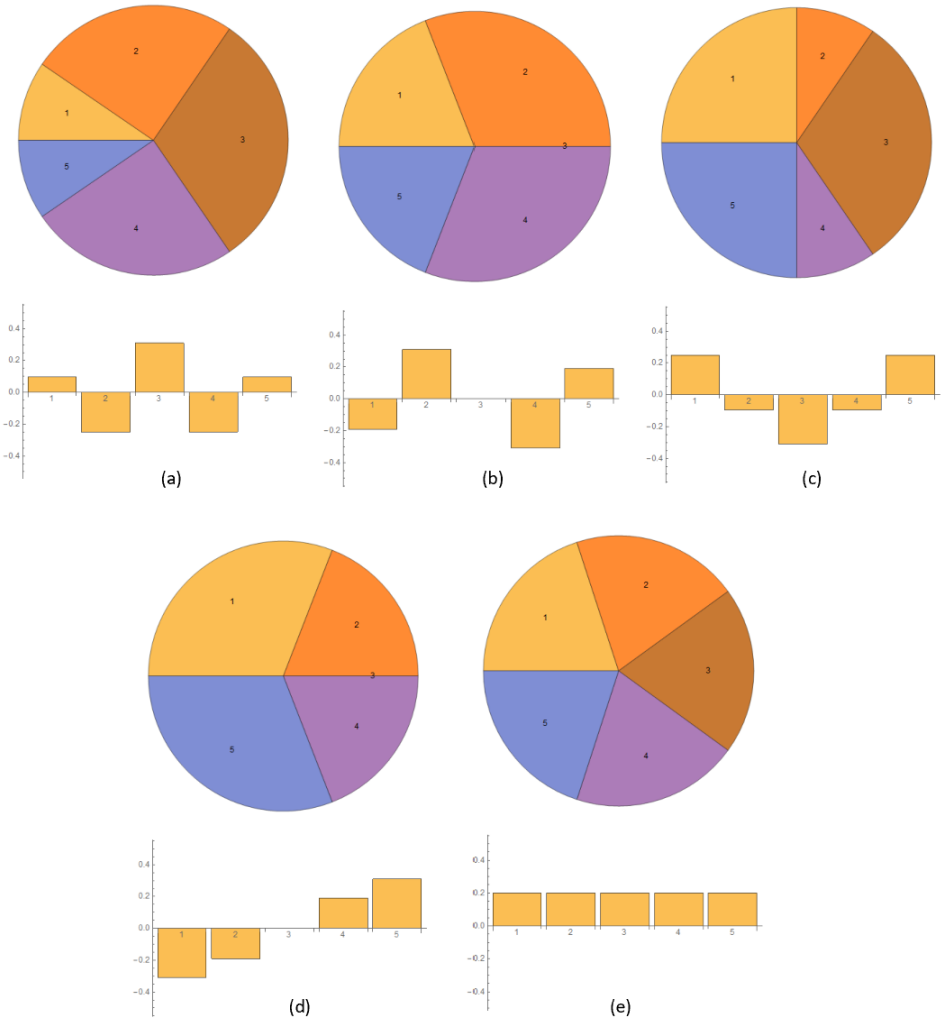

Figure 25: Visual illustration of the weighting within different currents, each weight is associated to an eigenvector from matrix b, taken from the columns of matrix U^{-1}, for a system with $n = 5$. Base associated to current is shown from (a) $\boldsymbol{i}_5$ to (e) $\boldsymbol{i}_1$,

One could expect finding a bigger contribution of the biggest or smallest values within the linear combinations, however, from Figure.25 there is not any clear pattern or dominance but apparently if total contributions are taken into account by summing up each chart they all contribute equally. It is indeed interesting that $\boldsymbol{i}_1$ has equal positive contributions from all eigenvectors.

To end with, and as further consideration, we are interested in not only the set up in which $r = 1$ but also into different ones for which value of r gets closer to 0.01. Therefore, some simulations for these values are included in Figures.26,27 where we can actually see that for smaller values of r different i get closer until they become all the same.

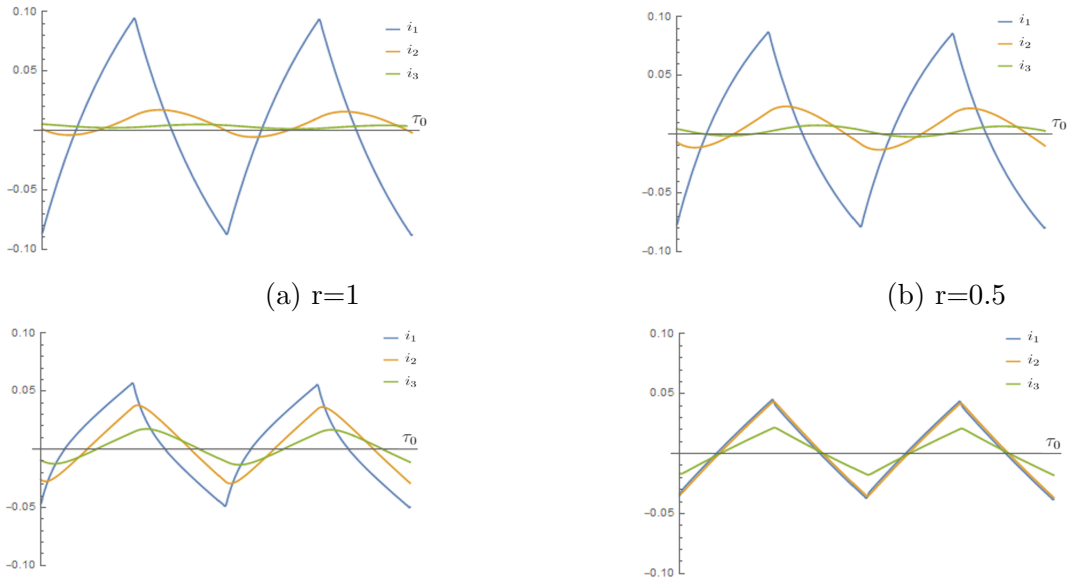

(a) r=1 (b) r=0.5

(c) r=0.1 (d) r=0.01

Figure 26: Dimensionless current $\frac{i}{5\theta C}$ vs $\frac{t}{t_0}$ using the solution of the RC circuit being n=3 for $\alpha = 1$ and different values of r with $m_{max} = 51$. In this plot $\sum_k^n i$ is not included due to the fact it wouldn't be able to distinguish any differences among the currents.

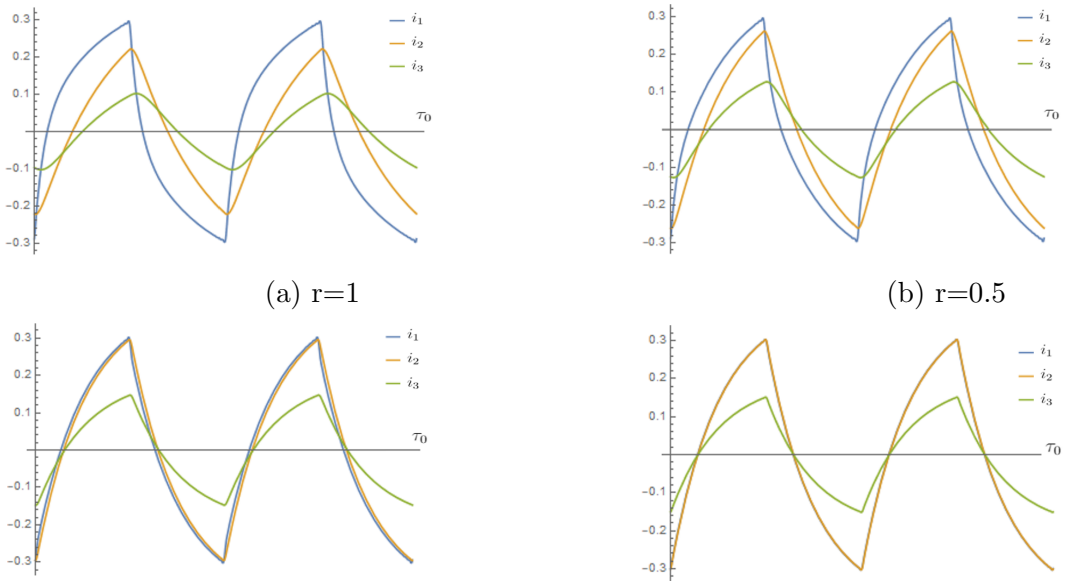

(a) r=1 (b) r=0.5

(c) r=0.1 (d) r=0.01

Figure 27: Dimensionless current $\frac{i}{5\theta C}$ vs $\frac{t}{t_0}$ using the solution of the RC circuit being n=3 for $\alpha = 0.1$ with different values of r and $m_{max} = 51$.In this graph $\sum_k^n i$ is not included due to the fact it wouldn't be able to distinguish any differences among the currents

5 Conclusions and discussion.

In this thesis we studied the charging dynamics of the supercapacitor using the multiple stack electrode-electrolyte model.

To begin with, in the first approach with the single-plate capacitor, we found out how to solve analytically the PNP equations by making several assumptions. Thereby, solutions have turned out to be quite limited: small applied electrode potential,(i.e,in the linear regime) and for electrode-stack separation much larger than the Debye length (i.e, $\kappa^{-1} \ll L$) which means that we are actually operating in time-scales close to RC time. These assumptions although valid, brings with them some clear limitations within the study of supercapacitors, for instance, the geometry of the set up and their real applicability, as they usually operate at higher voltage. For those reasons, we believe although it is interesting procedure to follow, it might not be as useful as numerical solving methods, where a wide range of conditions could be analysed. Moreover, within the obtained results, the fact that for bigger values of the electrode separation, thus, closer to RC time-scale, we obtain a faster charging process (Figure.4) is indeed unexpected.

Next, from the solution, Eq.(30), of the proposed RC circuit model from Figure.5 we showed that the charging process was indeed RC time and have similar behaviour from the one predicted by the analytical solution. Right after that, we analyzed the stack model system under a time dependent potential using the same RC equilibrium model. In the absence of numerical data or analytical solutions to PNP equations for any given t dependent potential to compare with, we have to focus on the understanding of our results. On th one hand, for $t_0 \ll t_{RC}$ applied potential would be an incredibly fast oscillating function, which in the limit, would became sudden switching on and off, therefore, no EDL would have time to form. On the other hand, for $t_{RC} \ll t_0$ we would adiabatically change the potential,i.e., through infinitesimal changes along equilibrium states and in such case, each equilibrium point is linked to a stable EDL. Hence, values $\alpha \in [0.01, 10]$ are studied within the thesis. As a final remark, we can see in Figure.21 how the amplitude of the dimensionless current $\frac{I}{(5\theta C}$ decreases for a bigger value of the "coupling constant",i.e., $t_0 \approx t_{RC}$.

Regarding to the general n stack problem within the analytical solution frame, one of the main topics to discuss about are the proposed different time-scales. Figures.16,17 are indeed interesting, since we estimate that for a real system r would have a value close to 0.01. So even though we don't really understand the origin of the proposed Eq.(54) we can actually check that in both limits the behaviour is properly defined.

One interesting thing about the general RC circuit model is that we can actually change the geometry by varying the parameter labeled as $r = \frac{h}{L}$. The rest of this circuit,i.e., the resistances, capacitances and number of branches in the circuit model are not fit parameters but physically determined by our microscopic model. By doing so, we have actually checked how all the branches of the circuit tend to the same amplitude with the only exemption of the outer one which is different due to the imposed boundary condition to enclose the system.

Besides, we believe that one of the main contributions of this thesis might be the solution, Eq.(68), to the matrix differential equation from RC circuit Eq.(58) because it provides the solution to a general n stack model for any given form of the applied potential. I managed to derive it myself at the same time as my supervisor came across it using completely different methods. Nonetheless, I believe that one of the main gaps of this thesis is the absence of numerical data to compare with. Due to the corona-crisis we had some issues when connecting to the supercomputer of the university and therefore it was not available. I personally think it would have been the perfect complement for this thesis to strengthen the results obtained. However, we are quite optimistic about them due to the calculations done before by one of my supervisor Cheng Lian, which: "At small applied potentials, numerical simulations of the PNP equations are reproduced accurately by an equivalent circuit model." [13]. Thereby, data suggest that we are indeed in the correct path to follow.

5.1 Outlook

In future works, it is important that some points that have not been fully answered within this thesis are investigated,

- Undoubtedly more work needs to be done to understand the charging dynamics of porous capacitors regarding to finite ion sizes effects, more realistic modeling of pore morphology, position-dependent diffusion coefficients etc.
- Once the solution for the time dependent potential is known, further simulations with different applied potential could be done in order to compare with the triangular one chosen in the thesis.
- Regarding time scales discussed above there is still an very interesting open debate.
- More PNP calculations for bigger potentials and varying parameters to compare with the available experimental data.
- For the step potential charging process has been taken into account but not the discharging one once switched off.
- Study deeply a more accurate model to real system, i.e., increase the number of parallel plates with $r \approx 0.01$.
- Deeper analysis into the relation between eigenvectors and their combinations to get the weight-factors for the different currents. Good understanding of this algebraic relations might lead to finding out if there is any mode that makes the system go into resonance.

6 Acknowledgment

First of all I would like to thank Prof. Dr. René Van Roij for not only the time invested in this thesis but also for making me feel comfortable from the very first moment. Likewise, I deeply thank Dr. Cheng Lian for his good advises in our several meetings and discussions. Us three have created a well-coordinated team, overcoming this especially difficult times with the Corona-crisis, which I feel proud to be part of. Finally I would like to also thank to the Institute for Theoretical Physics, especially to the Soft Condensed Matter research group, for providing amazing means that enabled the enjoy of my research. Regarding to the thesis itself, I have to say that has been an exciting experience that fully met my expectations of how would it be to carry out a research project in a prestigious foreign university and I have checked myself what one teacher once told me, that the most difficult thing in physics was to come up with the adequate questions, thus, making a small contribution to science.

"Caminante no hay camino, se hace camino al andar" (Walker, there is no path to follow, you make the path by walking),

References

[1] J. Miller, Battery+ Energy Storage Technology p. 61 (2007).

[2] H. I. Becker, *Low voltage electrolytic capacitor* (1957), uS Patent 2,800,616.

[3] J. Ho, T. R. Jow, and S. Boggs, IEEE Electrical Insulation Magazine **26**, 20 (2010).

[4] R. De Levie, Electrochimica Acta **8**, 751 (1963).

[5] L. Helseth, Journal of Energy Storage **25**, 100912 (2019).

[6] M. Mirzadeh, F. Gibou, and T. M. Squires, Physical review letters **113**, 097701 (2014).

[7] G. Feng and P. T. Cummings, The Journal of Physical Chemistry Letters **2**, 2859 (2011).

[8] C. Péan, C. Merlet, B. Rotenberg, P. A. Madden, P.-L. Taberna, B. Daffos, M. Salanne, and P. Simon, ACS nano **8**, 1576 (2014).

[9] C. Noh and Y. Jung, Physical Chemistry Chemical Physics **21**, 6790 (2019).

[10] A. Chatterji and J. Horbach, The Journal of chemical physics **126**, 064907 (2007).

[11] C. Lian, S. Zhao, H. Liu, and J. Wu, The Journal of chemical physics **145**, 204707 (2016).

[12] A. Ambrozevich, S. Ambrozevich, R. Sibatov, and V. Uchaikin, Russian Electrical Engineering **89**, 64 (2018).

[13] C. Lian, M. Janssen, H. Liu, and R. van Roij, Phys. Rev. Lett. **124**, 076001 (2020), URL `https://link.aps.org/doi/10.1103/PhysRevLett.124.076001`.

[14] R. V. Roij, *Lecture notes for soft condensed matter theory* (2010).

[15] P. Kouyzer, *Master's thesis, charging dynamics in nanoporous electrodes* (2015).

[16] K. F. Riley, M. P. Hobson, and S. J. Bence, *Mathematical methods for physics and engineering: a comprehensive guide* (Cambridge university press, 2006).

[17] H. Wang, A. Thiele, and L. Pilon, The Journal of Physical Chemistry C **117**, 18286 (2013).

A Appendix

A.1 Solution to PNP equation for the single-plate capacitor

In this first section of the appendix we give a detailed description of how PNP equations are solved for the simple case.

$$\begin{aligned}
\partial_z^2\phi(z^*,\tau) &= -\frac{\rho_e(z^*,\tau)}{\lambda^2},\\
\partial_\tau\rho_{e,c}(z^*,\tau) &= -\lambda\partial_{z^*}j_{e,c}(z^*,\tau),\\
j_e(z^*,\tau) &= -(\partial_{z^*}\rho_e(z^*,\tau) + c(z^*,\tau)\partial_{z^*}\phi(z^*,\tau)),\\
j_c(z^*,\tau) &= -(\partial_{z^*}c(z^*,\tau) + \rho_e(z^*,\tau)\partial_{z^*}\phi(z^*,\tau)),\\
j_{e,c}(\pm1,\tau) &= 0,\\
\phi(\pm1,\tau) &= \mp\Phi_0.
\end{aligned}$$

Under assumption of small potential $\Phi_0 << 1$, then $c \approx 1$, and joining first three equations above the following differential equation is obtained, while boundary conditions are maintained:

$$\frac{\partial\rho_e(z^*,\tau)}{\partial\tau} = \lambda\frac{\partial^2\rho_e(z^*,\tau)}{\partial z^{*2}} - \frac{1}{\lambda}\rho_e(z^*,\tau). \tag{71}$$

By using the methods I describe in Appendix A in Laplacean space eq. transforms as

$$s\overline{\rho_e}(z^*,s) - \rho_e(z^*,0) = \lambda\frac{d^2\overline{\rho_e}(z^*,s)}{dz^{*2}} - \frac{1}{\lambda}\overline{\rho_e}(z^*,s). \tag{72}$$

Note that the relative ionic density evaluated in $t = 0$ is null because $\rho_-(z^*,0) = \rho_+(z^*,0)$. Then, Eq.(20) becomes:

$$\frac{d^2\overline{\rho_e}(z^*,s)}{dz^{*2}} = k^2\overline{\rho_e}(z^*,s), \tag{73}$$

where $k^2 = \frac{1}{\lambda^2}(1+s\lambda)$. Solutions are straightforward and applying the fact that we require to be anti symmetric, i.e, $B(s) = 0$, our solution,

$$\overline{\rho_e}(z^*,s) = A(s)\sinh kz^*. \tag{74}$$

where $A(s)$ is explicitly shown in Apppendix A since I consider it's not essential for the understanding of the derivation by now it's enough to know it's a function of s. Boundary conditions have to be transformed as well to the Laplacean space,

$$\begin{aligned}
\overline{j_e}(\pm1,s) &= 0,\\
\overline{\phi}(\pm1,s) &= \mp\frac{\Phi_0}{s}.
\end{aligned}$$

In order to solve this non trivial set of equations Laplace transform can be used due to the fact that can replace a PDE with an ODE which is easy to solve in Laplacean space. Let us

first introduce useful notation similar to the one used in the book *Mathematical Methods for Physics and Engineering* [16].

$$L[f(z^*,\tau)] = \int_0^\infty e^{-s\tau} f(z^*,\tau)d\tau = \overline{f}(z^*,s)$$

Following properties are well known:

1. $L[\frac{\partial f(z^*,\tau)}{\partial \tau}] = s\overline{f}(z^*,s) - f(z^*,0)$.
2. $L[\frac{\partial f(z^*,\tau)}{\partial z^*}] = \frac{d\overline{f}(z^*,\tau)}{dz^*}$.
3. $L[\frac{\partial^2 f(z^*,\tau)}{\partial {z^*}^2}] = \frac{d^2\overline{f}(z^*,\tau)}{d{z^*}^2}$. Solution obtained can be actually integrate from negative spatial boundary to any point in the space ($z^* \in [-1,1]$) and using (21). (Note that due to symmetry $\sinh \pm k = \pm \sinh k$ and $\cosh \pm k = \cosh k$)

$$\lambda^2 \int_{-1}^{z^*} \partial_{z^*}^2 \overline{\phi}(z^*,s)dz^* = A(s) \int_{-1}^{z^*} \sinh(kz^*)dz^*$$

$$-\lambda^2[\partial_{z^*}\phi(z^*,s)) - \partial_{z^*}\phi(-1,s)] = \frac{A(s)}{k}[\cosh(kz^*) - \cosh(k)]$$

First boundary condition can be applied using eq.

$$\overline{j_e}(\pm 1,s) = 0 = -[\partial_{z^*}\overline{\rho_e}(\pm 1,s) + \partial_{z^*}\overline{\phi}(\pm 1,s)],$$

$$\left.\frac{\partial \overline{\rho_e}(z^*,s)}{\partial z^*}\right|_{(\pm 1,s)} = A(s)k\cosh(kz^*)\Big|_{\pm 1} = A(s)k\cosh(k)$$

Using these previous equations we get the second boundary condition

$$\partial_{z^*}\overline{\phi}(\pm 1,s) = -A(s)k\cosh(k),$$

Therefore by substitution the differential equation for effective potential in laplacian space

$$-\lambda^2\partial_{z^*}\overline{\phi}(z^*,s)) = \frac{A(s)}{k}\cosh(kz^*) + \Xi(s)$$

with $\Xi(s) = A(s)k\cosh(k)[\lambda^2 - \frac{1}{k^2}]$ which makes equation visually easier. By integrating once again

$$-\lambda^2[\overline{\phi}(z^*,s) - \overline{\phi}(\pm 1,s)] = \Xi(s)[z^* - (\pm 1)] + \frac{A(s)}{k^2}[\sinh kz^* - (\pm \sinh k)].$$

$$-\lambda^2\overline{\phi}(z^*,s) \mp \lambda^2\frac{\Phi_0}{s}] = \Xi(s)[z^* \mp 1)] + \frac{A(s)}{k^2}[\sinh kz^* \mp \sinh k)].$$

Subtracting both solutions, form of $A(s)$ is achieved, taking into account the fact that $\lambda^2 - k^{-2} = k^{-2}s\lambda$:

$$A(s) = \frac{\Phi_0 s^{-1}\lambda^2 k^2}{\sinh k + s\lambda k \cosh k}. \tag{75}$$

Finally expression for the Laplacian effective potential is given by the sum of both solutions,

$$\overline{\phi}(z^*, s) = -\frac{A(s)}{\lambda^2 k^2}[\sinh kz^* + sz^*\lambda k \cosh k]. \tag{76}$$

One of the most interesting things to do now that we have the solution is to study how surface charge varies over time. Eq.(10) can rewritten using eq.1 setofeq directly in the s space the dimensionless charge density $\sigma^*(\tau) = \frac{\kappa}{\rho_b}\sigma(\tau)$,

$$\overline{\sigma^*}(s) = \frac{1}{\lambda}\int_{-1}^{1} \overline{\rho_e}(z^*, s)dz^*.$$

and by using 75 and 76

$$\overline{\sigma^*}(s) = -\frac{A(s)}{\lambda}\int_{-1}^{1} \sinh kz^* dz^* = \frac{2A(s)}{k\lambda}(1 - \cosh k). \tag{77}$$

However, carrying out the inverse Laplace transform is extremely hard so we must, for simplicity, make another assumption. To do so, it might be useful to introduce the so called Debye time, defined as $t_D = \kappa^{-2}L^{-1}$, which is the time it takes for an ion to make a displacement of Debye length (κ) due to the Brownian motion carried out by diffusion.We can imagine the initial state just before voltage is set, when ions are homogeneously distributed within the electrolyte. t_D right after voltage is on, some neighbour ions might have swapped their position, however, neutrality is maintained because voltage had no time change. In other words, system shows little reaction for $t_D \gg t$.
Therefore $t \gg t_D$ can be considered, which translated to dimensionless quantities defined before by doing few changes $t\frac{\kappa D}{L} \gg \frac{1}{\kappa L}$ are :

$$\tau \gg \lambda.$$

In s space , $L[\tau] \gg L[\lambda]$ which is $\frac{1}{s^2} \gg \frac{\lambda}{s}$

$$1 \gg s\lambda. \tag{78}$$

?? can be actually used in order to carry out a Taylor expansion around $s\lambda = 0$

$$\overline{\sigma^*}(s) = \frac{K_{\sigma^*}s^{-1}}{1 + s\tau_{\sigma^*}}, \tag{79}$$

where

$$K_{\sigma^*} = \frac{-2\Phi_0[1-(\lambda^{-1})]}{\tanh\lambda^{-1}},$$
$$\tau_{\sigma^*} = \frac{1+\frac{1}{2}(\lambda^{-1})^2}{\tanh(\lambda^{-1})} - \frac{\lambda}{2} - \frac{\tanh\lambda^{-1}(\lambda^{-1})}{2(1-(\lambda^{-1})},$$

By using tables, inverse for Eq.(25) is indeed straightforward, $L^{-1}[\frac{s^{-1}}{1+\tau_0 s}] = 1 - e^{\frac{\tau}{\tau_0}}$

$$\sigma^*(\tau) = K_{\sigma^*}(1 - e^{-\frac{\tau}{\tau_{\sigma^*}}}).$$

Which is the solution we were looking for.

A.2 Solution to differential equation

In this section we give a solution to a linear differential equation for the simple case, that will then be useful in order to solve general time dependent solution.
Differential equation for the RC model with a non constant potential:

$$\Delta\dot{\Psi}(t) + \frac{1}{t_{RC}}\Delta\Psi(t) = \frac{1}{t_{RC}}\Psi(t),$$
$$\Delta\Psi(t=0) = 0.$$

This is a linear differential equation of the form,

$$x^{'}(t) + bx(t) = f(t).$$

We can always multiply this equation by this function:

$$\mu(t) = e^{\int b(t)dt}.$$

So the linear equation becomes,

$$[\mu(t)x(t)]' = \mu(t)f(t),$$
$$x(t) - x(t=0) = \frac{1}{\mu(t)}\int_0^t \mu(t)f(t) = e^{-bt}\int_0^t f(t)e^{bt}dt. \tag{80}$$

Thus, solution to the equation is given by:

$$\Delta\Psi(t) = \frac{1}{t_{RC}}e^{-\frac{t}{t_{RC}}}\int_0^t \Psi(t)e^{\frac{t}{t_{RC}}}dt. \tag{81}$$

A.3 Integrating final solution

In this section we show how to integrate towards the solution. First term of the integral is straightforward, however, this one is not. Once we know the Fourier transform of the applied potential general solution is given substituting into Eq.(33),

$$\Delta\Psi(t) = \frac{\Psi_0}{t_{RC}} e^{-\frac{t}{t_{RC}}} \left[\int_0^t \left[\frac{1}{2} - \frac{4}{\pi^2} \sum_{m=1,3,5...}^{\infty} \frac{1}{m^2} \cos\left(\frac{m\pi}{t_0} t \right) \right] e^{\frac{t}{t_{RC}}} dt \right]. \tag{82}$$

For carrying out this integral we take for simplicity $\lambda = t_{RC}^{-1}$ and $\omega = \frac{m\pi}{t_0}$, so it is solved by

$$\int_0^t \cos(\omega t) e^{\lambda t} dt = \frac{e^{\lambda t} \left[\lambda \cos(\omega t) + \omega \sin(\omega t) \right] - \lambda}{\lambda^2 + \omega^2} \tag{83}$$

Finally, solution leads to

$$\Delta\Psi(t) = \Psi_0 \left[\frac{(1 - e^{-\lambda t})}{2} - \frac{4}{\pi^2} \sum_{m}^{\infty} \frac{\lambda}{m^2} \frac{\left(\lambda \cos(\omega t) + \omega \sin(\omega t) - \lambda e^{-\lambda t} \right)}{\lambda^2 + \omega^2} \right]. \tag{84}$$

A.4 General solutions to the step-function potential

More plots of the results of the analytical solutions of the PNP equations are included in this appendix:

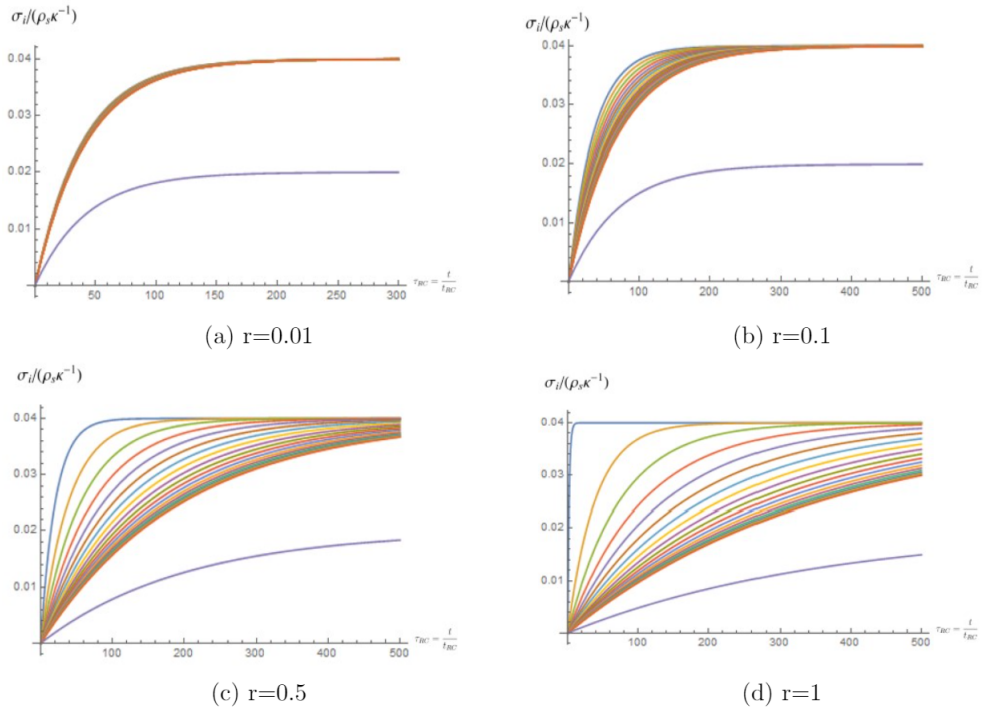

(a) r=0.01 (b) r=0.1

(c) r=0.5 (d) r=1

Figure 28: Dimensionless surface charge plotted vs $\frac{t}{t_{RC}}$ using the analytical solution to PNP equations for the general model and time scale described in Eq.(54) for $\Phi_0 = 0.01$ and $\lambda = 0.01$ being n=20.

Using the results from the RC circuit model:

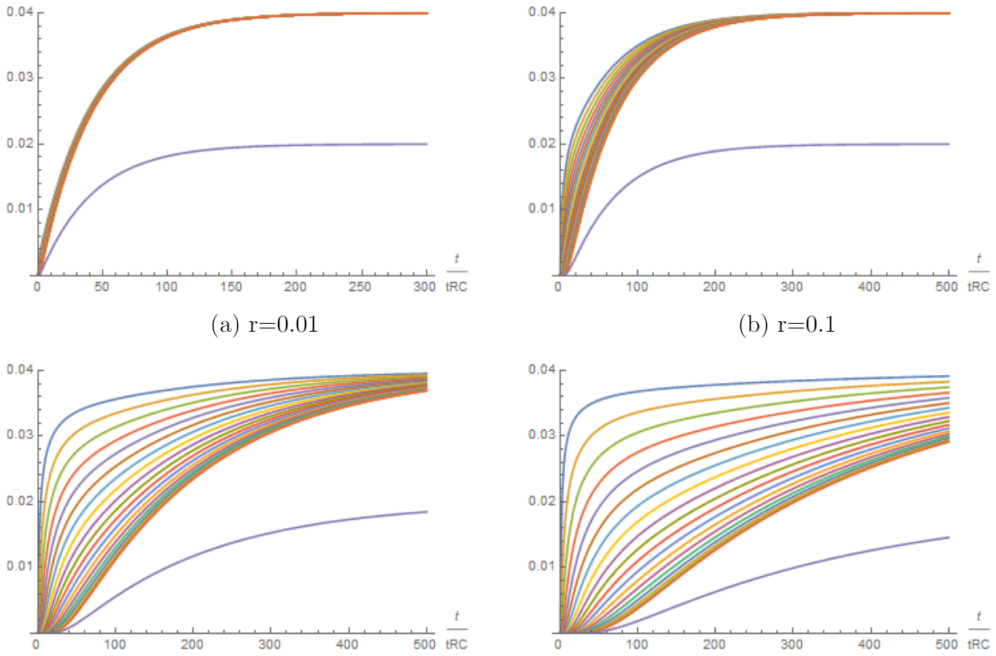

(a) r=0.01 (b) r=0.1

(c) r=0.5 (d) r=1

Figure 29: Dimensionless surface charge plotted vs $\frac{t}{t_{RC}}$ using the results from the RC circuit model weighted with $\frac{1}{50}$ for $\Phi_0 = 0.01$ and $\lambda = 0.01$ being n=20.

Apparently, by looking to Figures.28, 29 surface charge rates show a identical behaviour for small values of r while the charging process of the RC is, in general, faster than the analytical ones with the exception of the blue lines for $r = 1$, i.e., the inner capacitor.

A.5 Solutions to time-dependent potential

More plots for the time-dependent solutions are included in this last part of the appendix

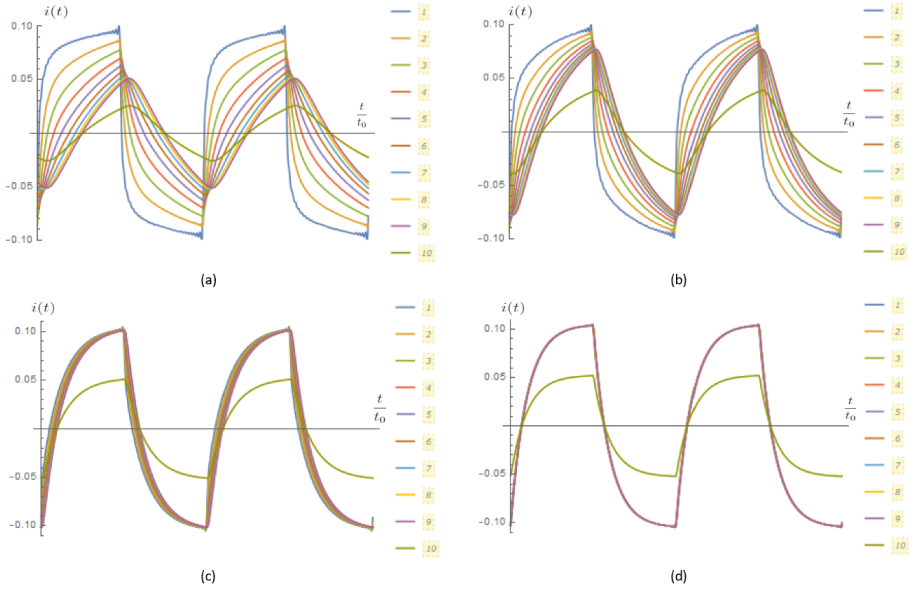

Figure 30: Two periods of the dimensionles current, $\frac{I}{19\theta C}$, plotted vs $\frac{t}{t_0}$ using the solution to time-dependent potential for the equivalent RC circuit model with n=10 and $\alpha = 0.01$.

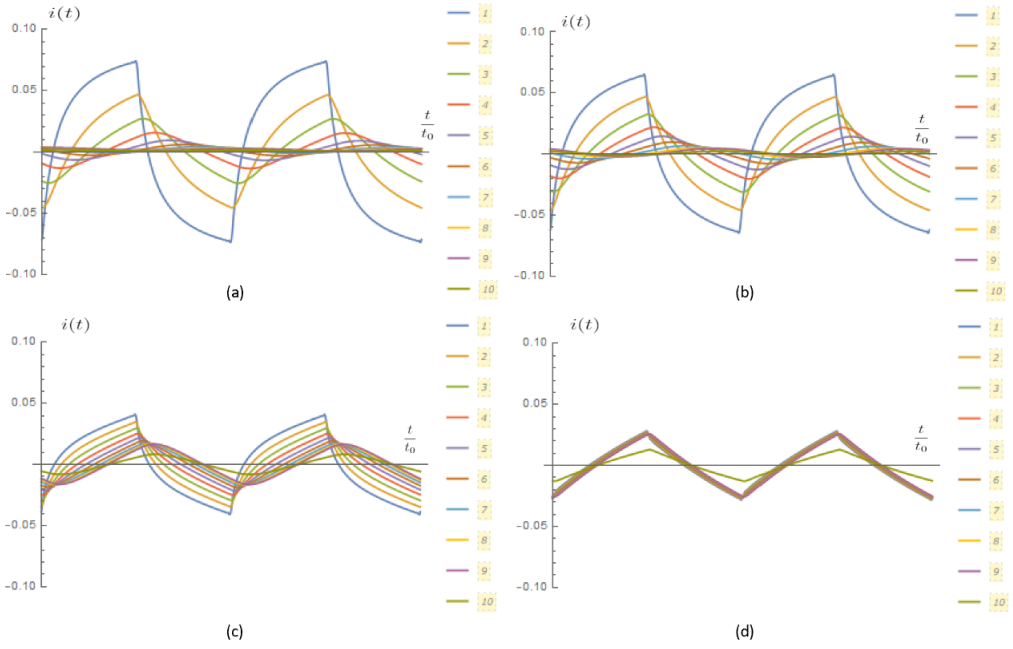

Figure 31: Two periods of the dimensionles current, $\frac{I}{19\theta C}$, plotted vs $\frac{t}{t_0}$ using the solution to time-dependent potential for the equivalent RC circuit model with n=10 and $\alpha = 0.1$.